Bioorganic & Medicinal Chemistry 19 (2011) 2269–2281

Contents lists available at ScienceDirect

Bioorganic & Medicinal Chemistry

journal homepage: www.elsevier.com/locate/bmc

Design, synthesis and structure–activity relationship (SAR) studies of 2,4-disubstituted pyrimidine derivatives: Dual activity as cholinesterase and Aβ-aggregation inhibitors

Tarek Mohamed [a,b], Xiaobei Zhao [c], Lila K. Habib [d], Jerry Yang [c], Praveen P. N. Rao [b,*]

[a] Department of Biology, University of Waterloo, Waterloo, Ontario, Canada
[b] School of Pharmacy, Health Sciences Campus, University of Waterloo, Waterloo, Ontario, Canada N2L 3G1
[c] Department of Chemistry and Biochemistry, University of California, San Diego, 9500 Gilman Drive, La Jolla, CA 92093-0358, USA
[d] Department of Bioengineering, University of California, San Diego, 9500 Gilman Drive, La Jolla, CA 92093-0358, USA

ARTICLE INFO

Article history:
Received 6 December 2010
Revised 11 February 2011
Accepted 16 February 2011
Available online 1 March 2011

Keywords:
Cholinesterase inhibitors (ChEIs)
Acetylcholinesterase (AChE)
Butyrylcholinesterase (BuChE)
Human acetylcholinesterase (*h*AChE)
Structure–activity relationship (SAR)
Amyloid-β (Aβ)
5,5′-Dithiobis(2-nitrobenzoic acid) (DTNB)
Thioflavin T (ThT)
3-(4,5-Dimethylthiazol-2-yl)-2,5-diphenyl tetrazolium bromide (MTT)

ABSTRACT

A novel class of 2,4-disubstituted pyrimidines (**7a–u**, **8a–f**, **9a–e**) that possess substituents with varying steric and electronic properties at the C-2 and C-4 positions, were designed, synthesized and evaluated as dual cholinesterase and amyloid-β (Aβ)-aggregation inhibitors. In vitro screening identified *N*-(naphth-1-ylmethyl)-2-(pyrrolidin-1-yl)pyrimidin-4-amine (**9a**) as the most potent AChE inhibitor (IC_{50} = 5.5 μM). Among this class of compounds, 2-(4-methylpiperidin-1-yl)-*N*-(naphth-1-ylmethyl)pyrimidin-4-amine (**9e**) was identified as the most potent and selective BuChE inhibitor (IC_{50} = 2.2 μM, selectivity index = 11.7) and was about 5.7-fold more potent compared to the commercial, approved reference drug galanthamine (BuChE IC_{50} = 12.6 μM). In addition, the selective AChE inhibitor *N*-benzyl-2-(4-methylpiperazin-1-yl)pyrimidin-4-amine (**7d**), exhibited good inhibition of *h*AChE-induced aggregation of $A\beta_{1-40}$ fibrils (59% inhibition). Furthermore, molecular modeling studies indicate that a central pyrimidine ring serves as a suitable template to develop dual inhibitors of cholinesterase and AChE-induced Aβ aggregation thereby targeting multiple pathological routes in AD.

1. Introduction

Neurological disorders inflict a heavy burden on healthcare costs, affected individuals and their caregivers. Alzheimer's disease (AD) is classified as a progressive, neurodegenerative disease that affects the cholinergic regions of the central nervous system (CNS) that associate with cognitive function and spatial awareness.[1] This devastating neurological disease targets the elderly populations and its prevalence is on the rise.[2,3] The hallmark characteristics of AD include the rapid loss of cholinergic neurotransmission, accelerated aggregation of amyloid-β (Aβ) peptides and formation of neurofibrillary tangles (NFTs) of hyperphosphorylated tau protein.[2–6] These characteristics establish the basis for the cholinergic, amyloid and tau hypotheses for AD pathology, respectively.

According to the cholinergic hypothesis, the pathology of AD is attributed to the rapid decline in neurotransmission in the cholinergic regions of the CNS that house acetylcholine (ACh) utilizing sympathetic and parasympathetic neurons.[7] The acetyl and butyrylcholinesterase (AChE and BuChE, respectively) enzymes act on ACh to terminate its actions in the synaptic cleft by hydrolyzing the neurotransmitter to choline and acetate.[8,9] Deficiencies in the ACh synthesizing enzyme (choline acetyltransferase—ChAT) also contributes to the overall decline of ACh concentration in the cortical regions of the brain.[9–12] Furthermore, recent studies have shown that the ratio of AChE to BuChE is dependent on the stage of pathogenesis. In the CNS, AChE plays a vital role in the early stages of AD. However, as the disease progresses and cholinergic neurons are depleted, BuChE, which has a wider distribution within the body, acts as the major degrading enzyme.[13,14]

In contrast, the amyloid hypothesis suggests that the progression of AD is attributed to the accelerated accumulation of toxic forms of self-induced and/or AChE-promoted toxic aggregates of Aβ peptides.[15–17] These toxic peptides arise from the cleavage of the amyloid-precursor protein (APP) by the β-secretase (BACE-1) and γ-secretase enzymes. In this regard, recent studies indicate a link between the cholinergic and amyloid hypotheses.[18,19] AChE is known to induce amyloid-β (Aβ) formation leading to the highly toxic AChE-Aβ peptide complexes.[20–22] These multiple factors in AD pathology mandate the need to develop small molecule thera-

* Corresponding author. Tel.: +1 519 888 4567x21317; fax: +1 519 888 7910.
E-mail address: praopera@uwaterloo.ca (P.P.N. Rao).

0968-0896/$ - see front matter © 2011 Elsevier Ltd. All rights reserved.
doi:10.1016/j.bmc.2011.02.030

pies that exhibit dual ChE inhibition as well as reduce the formation of neurotoxic Aβ-aggregates.

Research into the cholinergic hypothesis has led to the development of several fused and non-fused ring systems as ChE inhibitors (ChEIs) (Fig. 1). For example, tacrine (**1**), an acridine derivative, was one of the earliest ChEI developed to treat AD.[23] Bis-7-tacrine (**2**) is a potent dual AChE and BuChE inhibitor.[24] Propidium (**3**) binds specifically to the peripheral anionic site (PAS) of AChE.[25] The anti-Alzheimer drug donepezil (**4**), is highly selective toward AChE and its binding conformation spans both the catalytic and peripheral sites of AChE.[26] Recent work by DeLisa and co-workers examined *s*-triazine based ring templates (**5**) for their ability to inhibit the aggregation of $A\beta_{1-42}$ plaques.[27]

As part of our research program, we previously reported the development of a group of heterocyclic, non-fused ChEIs based on a 2,4-disubstituted pyrimidine ring template.[28] Here we report the design, synthesis and evaluation of heterocycles **7a**–**u**, **8a**–**f**, **9a**–**e** containing a 2,4-disubstituted pyrimidine ring scaffold as novel small molecules possessing dual activity as cholinesterase inhibitors and as inhibitors of *h*AChE-induced $A\beta_{1-40}$ aggregation.

2. Results and discussion

2.1. Chemistry

The synthesis of target 2,4-disubstituted pyrimidine derivatives (**7a**–**r**, **8a**–**f** and **9a**–**e**) was accomplished in two steps. In the first step, the *N*-benzyl, *N*-phenethyl and naphth-1-ylmethyl-2-chloropyrimidin-4-amine intermediates (**7**, **8** and **9**, respectively) were synthesized from the 2,4-dichloropyrimidine starting material (**6**) by a nucleophilic aromatic substitution reaction at C-4 using a base such as *N*,*N*-diisopropylethylamine (DIPEA). The reaction was run in EtOH at 75–85 °C and refluxed for 3 h. The intermediates **7**, **8** and **9** were obtained in moderate to good yield ranging from 60% to 75% (Scheme 1).[28,29]

In the second step, the C-2 chlorine was displaced by various cyclic amines (R^2 = pyrrolidine, morpholine, thiomorpholine, 1-methylpiperazine, 4-methylpiperidine, acetylpiperazine, *t*-butyl piperazine-1-carboxylate, cyclohexylpiperazine, isopropylpiperazine, isopropylpiperidine, *N*-propylpiperazine, *N*-hydroxyethyl-piperazine, *N*-methoxyethylpiperazine, 4-chloro, bromo, fluoro and trifluoromethylbenzylpiperazine, 4-amino-1-benzylpiperidine, Scheme 1). This reaction was run under rigorous conditions

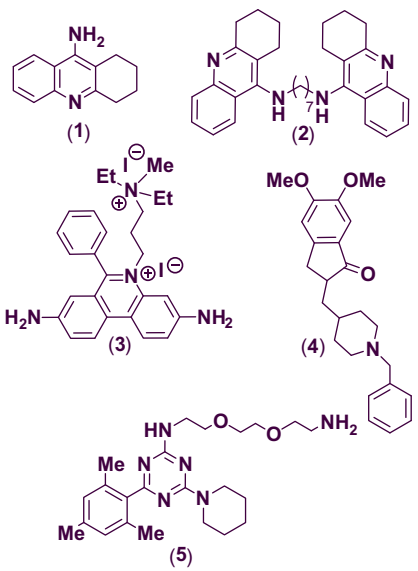

Figure 1. Structures of ChEIs (**1**, **2** and **4**) and inhibitors of Aβ-aggregation (**3** and **5**).

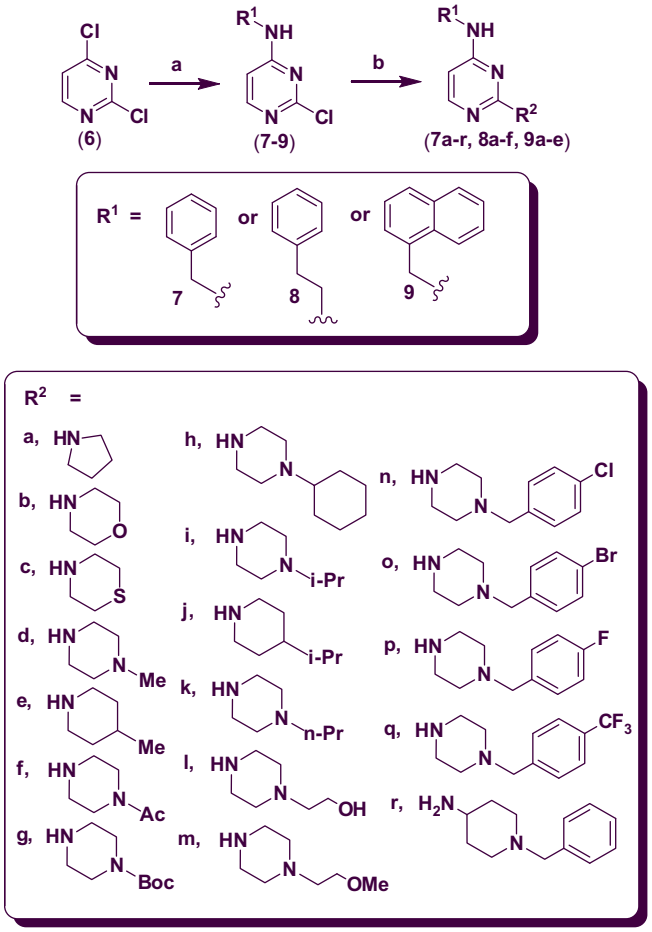

Scheme 1. Reagents and conditions: (a) DIPEA, phenylmethanamine (**7**), 2-phenylethanamine (**8**) or (naphthalene-1-yl)methanamine (**9**), EtOH, 0 °C to 75–85 °C and reflux for 3 h.; (b) R^2 = pyrrolidine, morpholine, thiomorpholine, 1-methylpiperazine, 4-methylpiperidine, acetylpiperazine, *t*-butyl piperazine-1-carboxylate, cyclohexylpiperazine, isopropyl piperazine, isopropylpiperidine, *N*-propylpiperazine, *N*-hydroxyethyl piperazine, *N*-methoxyethylpiperazine, 4-chloro, bromo, fluoro and trifluoromethylbenzylpiperazine, 4-amino-1-benzylpiperidine, *n*-BuOH, 145–150 °C, 30–40 min.

(145–150 °C) for 30–40 min in a sealed pressure vessel (PV) using *n*-butanol as a solvent to afford the target 2,4-disubstituted pyrimidine derivatives (**7a**–**r**, **8a**–**f**, **9a**–**e**) in moderate to good yield (50–90%) (Scheme 1).[28,30]

N-Benzyl-2-thiomorpholinopyrimidin-4-amine (**7c**) was oxidized to 4-[4-(benzylamino)pyrimidin-2-yl]thiomorpholine 1-oxide (**7s**) in good yield (75%) using *meta*-chloroperoxybenzoic acid (MCPBA) (Scheme 2) and to 4-[4-(benzylamino) pyrimidin-2-yl]thiomorpholine 1,1-dioxide (**7t**) in good yield (75%) using potassium peroxymonosulfate (Oxone®) as the oxidizing agent (Scheme 2).

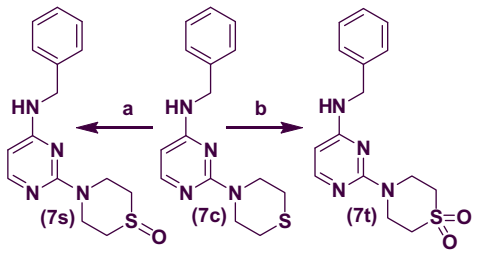

Scheme 2. Reagents and conditions: (a) *m*CPBA, **7c**, 1,4-dioxane, 0 °C to rt, 3 h; (b) Oxone®, **7c**, MeOH, H_2O and 1,4-dioxane, 0 °C to 70–75 °C, 1 h then rt, 4 h.

The deprotection of the *tert*-butoxycarbonyl (*t*-Boc) group of **7g** [*tert*-butyl 4-(4-(benzylamino)pyrimidin-2-yl)piperazine-1-carboxylate] was accomplished by using 50% *v/v* trifluoroacetic acid (TFA) to yield *N*-benzyl-2(piperazin-1-yl)pyrimidin-4-amine (**7u**) in good yield (75%) (Scheme 3).

2.2. Cholinesterase inhibition and SAR studies

The ability of the synthesized derivatives (**7a**–**u**, **8a**–**f** and **9a**–**e**) to inhibit both *h*AChE and equine BuChE was evaluated in vitro (IC_{50} values, Table 1).[28,31] Structure–activity relationship (SAR) studies indicated the cholinesterase inhibition and selectivity were sensitive to steric and electronic parameters at C-2 and C-4 positions of the central pyrimidine ring. They exhibited a broad range of inhibition (AChE IC_{50} = 5.5 to 28.8 μM range; BuChE IC_{50} = 2.2 to >100 μM range).

Among the *N*-benzyl series of derivatives (**7a**–**u**), the substituent electronic and steric factors at C-2 position modulated ChE inhibition. The presence of five-membered heterocycloalkyl C-2 substituent such as a pyrrolidine (**7a**) provided ChE inhibition with superior potency and selectivity toward AChE (AChE IC_{50} = 8.7 μM; BuChE IC_{50} = 26.4 μM). Replacing the C-2 with a six-membered morpholine provides **7b** that exhibited weak AChE (IC_{50} = 14 μM) and BuChE inhibition (IC_{50} = 68.3 μM) compared to **7a**. In contrast, the presence of a C-2 thiomorpholine ring in **7c** provided superior BuChE inhibition and selectivity (AChE IC_{50} = 23.2 μM; BuChE IC_{50} = 6.1 μM, SI = 3.8). This observation indicates that the differences in the electronic properties of oxygen and sulfur could modulate the binding modes within the active sites of both ChEs. This was further explored by oxidizing the sulfur in **7c** to either a sulfoxide (**7s**) or a sulfone (**7t**). Both **7s** and **7t** exhibited AChE inhibition, with **7s** exhibiting about 1.8-fold more potent AChE inhibition (IC_{50} = 12.6 μM) relative to **7c**. Interestingly, **7s** and **7t** (both lack the unsubstituted terminal sulfur atom present in **7c**) did not exhibit BuChE inhibition up to 100 μM.

The SAR of C-2 piperazine-substituted *N*-benzylpyrimidine derivatives were explored by incorporating a wide range of terminal 4-alkyl, alkoxy, acyl, cycloalkyl and substituted-benzyl rings (**7d, 7f**–**i, 7k**–**q**). The incorporation of terminal 4-alkylpiperazine and 4-alkoxy substituents (**7d, 7f**–**g**, **7i** and **7k**–**m**) provided AChE inhibition. The presence of a methyl group in **7d** (R^2 = 4-methylpiperazine) provided moderate AChE inhibition (IC_{50} = 24.9 μM), whereas increasing the chain length to propyl (**7k**, R^2 = 4-propylpiperazine) led to superior AChE inhibition (IC_{50} = 15.3 μM). In contrast, the presence of a branched, sterically demanding alkyl chain such as an isopropyl in **7i** (R^2 = 4-isopropylpiperazine) exhibited similar AChE inhibition (AChE IC_{50} = 25.0 μM) relative to **7d**. However, **7i** was a selective BuChE inhibitor (BuChE IC_{50} = 3.4 μM; SI = 7.35). Similarly, the presence of alkoxy groups such as hydroxyethyl in **7l** (AChE IC_{50} = 26.4 μM) or a methoxyethyl in **7m** (AChE IC_{50} = 26.7 μM) exhibited comparable AChE inhibition relative to **7d** (IC_{50} = 24.9 μM). Interestingly, C-2 piperazine R^2 substituents that possessed a terminal alkyl or alkoxy group (**7d, 7f**–**g** and **7k**–**m**) generally exhibited weak or a lack of BuChE inhibition (BuChE IC_{50} = 59.9 μM to >100 μM range) with the exception of **7i**. Furthermore, the unsubstituted C-2 piperazine containing compound **7u** exhibited selective AChE inhibition (IC_{50} = 15.5 μM) with no BuChE inhibition up to 100 μM. It was interesting to note that the presence of a cycloalkyl ring (**7h**) provided superior BuChE inhibition and selectivity (AChE IC_{50} = 22.9 μM; BuChE IC_{50} = 7.6 μM, SI = 3.01) among the piperazine derivatives. In contrast to terminal alkyl or alkoxy substituted piperazines, the presence of a C-2 benzylpiperazine possessing halogen atoms (Cl, Br or F) (**7n**–**p**) or electron withdrawing groups (CF_3) (**7q**) at the *para*-position exhibited dual ChE inhibition (AChE IC_{50} = 20.2 to 28.8 μM range; BuChE IC_{50} = 7.3 to 14.3 μM range) with the exception of **7q** (BuChE IC_{50} >100 μM). The AChE activity was of the order: Cl > F > Br > CF_3, whereas the presence of a fluorine atom at *para*-position provides superior BuChE inhibition (BuChE IC_{50} = 7.3 μM). The BuChE activity was of the order: F > Cl > Br > CF_3 (inactive at 100 μM) establishing the role of increasing electronegativity with superior BuChE inhibition. In addition, replacing the C-2 4-methylpiperazine (**7d**) with a methylpiperidine bioisostere in **7e** provided dual ChE inhibition along with superior BuChE inhibition and selectivity (AChE IC_{50} = 18.4 μM; BuChE IC_{50} = 3.4 μM, SI = 5.41) relative to **7d**. In addition to its superior BuChE inhibitory potency, **7e** was about 3.7-fold more potent relative to the reference drug galanthamine (BuChEIC_{50} = 12.6 μM), although it was not as potent as bis-tacrine (BuChEIC_{50} = 10 nM). Furthermore, the bioisosteric replacement of C-2 4-isopropylpiperazine in **7i** with an isopropylpiperidine bioisostere in **7j** provided dual ChE inhibition similar to **7i**, although with a 2.2-fold loss in BuChE inhibitory potency (BuChE IC_{50} = 6.5 μM) and a 1.7-fold gain in AChE inhibitory potency (AChE IC_{50} = 14.2 μM) compared to **7i**. In derivative **7r**, the benzylpiperidine pharmacophore present in donepezil was incorporated into a pyrimidine diamine template. This modification provided dual ChE inhibition and exhibited superior BuChE inhibition (BuChE IC_{50} = 8.2 μM) relative to the reference drug galanthamine (BuChE IC_{50} = 12.6 μM).

From the *N*-benzyl series (**7a**–**u**), **7a** was identified as the most potent AChE inhibitor (IC_{50} = 8.7 μM); **7s** as the most selective AChE inhibitor (SI <0.12); **7e** and **7i** as equally potent BuChE inhibitors (IC_{50} = 3.40 μM), where **7i** was also the most selective BuChE inhibitor (SI = 7.35).

In the *N*-phenethyl C-4 substituted pyrimidines (**8a**–**f**) evaluated, the presence of a five-membered pyrrolidine ring in **8a** led to dual ChE inhibition (AChE IC_{50} = 9.8 μM; BuChE IC_{50} = 13.8 μM) and similar dual ChE inhibition was seen with **8e** that possessed a six-membered methylpiperidine ring at C-2 (AChE IC_{50} = 8.8 μM; BuChE IC_{50} = 17.7 μM; Table 1). In contrast, the presence of C-2 six-membered rings such as morpholine (**8b**), thiomorpholine (**8c**), methylpiperazine (**8d**) and acetylpiperazine (**8f**) was detrimental to BuChE inhibition (IC_{50} values >100 μM; Table 1). It was interesting to note that the naphth-1-ylmethyl series of C-4 substituted pyrimidines (**9a**–**e**) evaluated exhibited dual ChE inhibition (AChE IC_{50} = 5.5 to 25.8 μM range; BuChE IC_{50} = 2.2 to 34.7 μM range; Table 1). For example, the presence of a C-2 five-membered pyrrolidine in **9a** provided superior BuChE inhibition (IC_{50} = 8.9 μM) relative to donepezil (BuChE IC_{50} = 12.6 μM) although it was a less potent AChE inhibitor relative to tacrine (AChE IC_{50} = 0.093 μM) or bis-tacrine (AChE IC_{50} = 4 nM). Replacing the C-2 five-membered pyrrolidine with either a six-membered morpholine (**9b**, AChE IC_{50} = 14.7 μM; BuChE IC_{50} = 28 μM) or thiomorpholine (**9c**, AChE IC_{50} = 12.8 μM; BuChE IC_{50} = 34.7 μM; Table 1) led to a decline in ChE inhibitory potency relative to **9a**. In contrast, the presence of either a C-2 4-methylpiperazine (**9d**) or the corresponding bioisostere methylpiperidine (**9e**) provided superior BuChE inhibitory potency and selectivity. Compound **9e** exhibited about 5.7-fold superior BuChE inhibition (IC_{50} = 2.2 μM) and selectivity

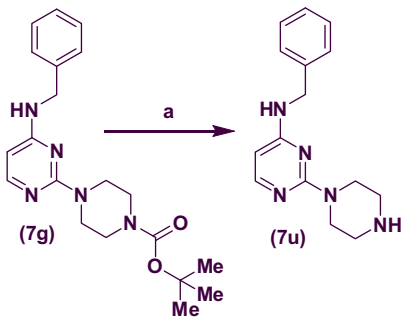

Scheme 3. Reagents and conditions: (a) TFA, **7g**, DCM, 0 °C to rt, 2 h.

Table 1
AChE and BuChE inhibitory activities and *C* log *P* data for 2,4-disubstituted pyrimidines (**7a–u**, **8a–f** and **9a–e**)

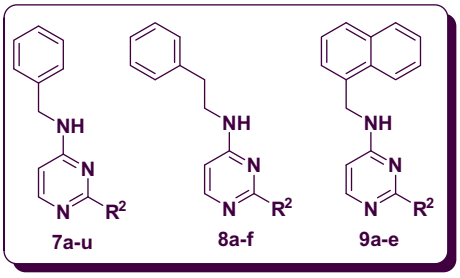

Compd	R^2	IC_{50}[a,b] (μM)		Selectivity index[b] (SI)	*C* log *P*[c]
		AChE	BuChE		
7a		8.70	26.40	0.33	2.97
7b	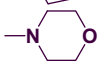	14.0	68.30	0.21	2.14
7c		23.20	6.10	3.80	2.98
7d		24.90	>100	<0.25	2.71
7e		18.40	3.40	5.41	4.05
7f	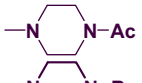	16.60	>100	<0.17	1.73
7g		18.80	>100	<0.19	4.12
7h	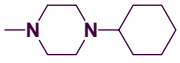	22.90	7.60	3.01	4.65
7i	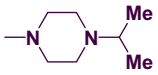	25.0	3.40	7.35	3.54
7j	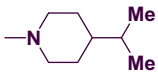	14.20	6.50	2.19	4.97
7k	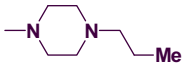	15.30	59.90	0.26	3.76
7l	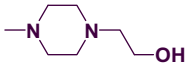	26.40	>100	<0.26	2.13
7m		26.70	>100	<0.27	2.89
7n	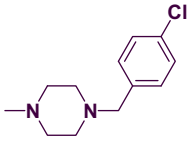	20.20	10.70	1.89	5.14
7o	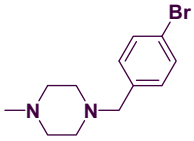	25.50	14.30	1.78	5.29
7p	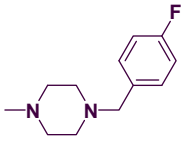	21.60	7.30	2.96	4.57

Table 1 (*continued*)

Compd	R^2	IC_{50}[a,b] (μM)		Selectivity index[b] (SI)	*C* log *P*[c]
		AChE	BuChE		
7q	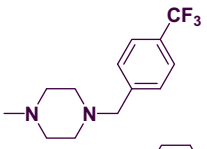	28.80	>100	<0.29	5.31
7r	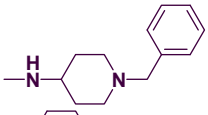	12.40	8.20	1.51	4.60
7s		12.60	>100	<0.13	1.26
7t		24.20	>100	<0.24	1.18
7u		15.50	>100	0.16	2.13
8a		9.80	13.80	0.71	3.62
8b		19.70	>100	<0.20	2.79
8c		26.40	>100	<0.26	3.63
8d		20.40	>100	<0.20	3.35
8e		8.80	17.70	0.50	4.69
8f		19.90	>100	<0.20	2.37
9a		5.50	8.90	0.62	4.14
9b		14.70	28.0	0.53	3.32
9c		12.80	34.70	0.37	4.15
9d	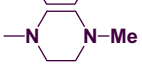	17.50	2.60	6.73	3.88
9e		25.80	2.20	11.73	5.22
Tacrine. HCl	Figure 1 (**1**)	0.093	0.019	9.11	3.27
Bis(7)-tacrine	Figure 1 (**2**)	0.004	0.010	0.171	10.10
Galanthamine·HBr	–	3.80	12.60	0.274	1.03
Donepezil. HCl		0.032	3.60		4.59

[a] The in vitro test compound concentration required to produce 50% inhibition of *h*AChE and equine BuChE.
[b] The result (IC_{50}) is the mean of two separate experiments ($n = 4$) and the deviation from the mean is <10% of the mean value. Selectivity index = *h*AChE IC_{50}/BuChE IC_{50}.
[c] *C* log *P* was determined using ChemDraw Ultra 12.0. CambridgeSoft Company.

(SI = 11.7) relative to the reference drug galanthamine (BuChE IC_{50} = 12.6 μM; SI = 0.27) and was much more potent compared to donepezil (BuChE IC_{50} = 3.6 μM) whereas the corresponding C-2 methylpiperidine **9d** exhibited similar BuChE inhibition (BuChE IC_{50} = 2.6 μM) and superior AChE inhibition (AChE IC_{50} = 17.5 μM) relative to **9e** (AChE IC_{50} = 25.8 μM). In addition, the theoretical partition coefficient values (*C* log *P*) of various synthesized pyrimidines (Table 1) compares well with the reference compound tacrine (*C* log *P* = 3.27) favoring their use as agents to treat disorders of the central nervous system (CNS).

2.3. Inhibition of *h*AChE-induced Aβ aggregation

Some 2,4-disubstituted pyrimidines that exhibit a range of cholinesterase inhibition activities (**7a, 7c, 7d, 7g, 7s, 7t, 8c** and **9c**) were evaluated to prevent *h*AChE-induced $A\beta_{1-40}$ aggregation by a thioflavin T (ThT) fluorescence method.[32] The anti-aggregating activity of eight 2,4-disubstituted pyrimidines along with reference compounds propidium iodide and donepezil are presented in Table 2. At a concentration of 100 μM, 2,4-disubstituted pyrimidines exhibited varying degrees of inhibition (inactive to 59% inhibition of aggregation). In compound **7a**, the presence of a smaller five-membered pyrrolidine at C-2 did not provide anti-aggregation activity (Table 2). Similarly, the presence of a C-2 thiomorpholine ring in **7c**, **8c** and **9c** provided either weak or no anti-aggregation activity. Among the 2,4-disubstituted pyrimidines evaluated, **7d** with a combination of C-4 *N*-benzyl and a C-2 methylpiperazine substituent exhibited good activity against *h*AChE-induced aggregation of $A\beta_{1-40}$ peptides (59% inhibition). This compound was 3.4-fold more potent compared to donepezil (17% inhibition) and was not as potent as propidium iodide (85% inhibition), which is known to bind to the PAS in AChE.[20,25] Interestingly, when the

Table 2
Inhibition of *h*AChE-induced aggregation of $A\beta_{1-40}$ by 2,4-disubstituted pyrimidines (**7a**, **7c**, **7d**, **7g**, **7s**, **7t**, **8c** and **9c**)

Compd	Inhibition at 100 μM ± SEM[a] (%)
7a	NA
7c	NA
7d	59.0 ± 2.9
7g	26.7 ± 17.0
7s	55.9 ± 6.3
7t	44.1 ± 11.0
8c	NA
9c	38 ± 25
Donepezil	17.4 ± 8.1
Propidium iodide	84.9 ± 4.1

[a] The values are the mean of two independent measurements each performed in triplicates, SEM = standard error of mean. NA = not active.

Table 3
MTT reduction cytotoxicity assay in SH-SY5Y neuroblastoma cells of 2,4-disubstituted pyrimidines (**7a**, **7c**, **7d**, **7g**, **7s**, **7t**, **8c** and **9c**)

Compd	Cell Viability at 40 μM ± SEM (%)[a]
7a	100.3 ± 16.4[b]
7c	97.8 ± 11.5
7d	98.3 ± 10.5
7g	102.3 ± 0.5[c]
7s	89.7 ± 11.5
7t	91.8 ± 2.2
8c	104.5 ± 4.6[d]
9c	89.3 ± 2.9
Tacrine	89.0 ± 6.3
Galanthamine	97.1 ± 12.9

[a] The values are the mean of measurements performed in quadruplicates, SEM = standard error of mean. 100% cell viability represents the viability of SH-SY5Y cells measured in the absence of small molecules, as determined by MTT reduction. Statistical analysis using an independent two-tailed student's *t*-tests were performed using Origin 7.0 (Microcal Software, Inc., Northhampton, MA) to evaluate the statistical significance of the difference between the viability of control cells (measured in the absence of test molecules) and experimental mean values. A *p*-value of <0.05 was defined as statistically significant.
[b] *p*-Value = 0.97.
[c] *p*-Value = 0.30.
[d] *p*-Value = 0.55.

C-2 thiomorpholine substituent of **7c** was oxidized to a polar sulfoxide (**7s**) or a sulfone (**7t**), it provided anti-aggregation activity of about 56% and 44% inhibition, respectively (Table 1). This suggests that small molecules with polar functional groups could potentially exhibit superior binding within the AChE active which has polar pockets in its catalytic site (Ser203, His447, Glu202) as well as the active site gorge entry (Trp286, Tyr124). This justifies our results that the presence of polar functional groups at C-2 in **7d**, **7s** and **7t** led to superior inhibition of AChE-promoted Aβ aggregation compared to **7g** that has a lipophilic boc group at C-2. These studies indicate that the substituent electronic and steric effects both at the C-2 and C-4 positions can be manipulated to develop 2,4-disubstituted pyrimidines that bind favorably within the PAS present in AChE. Further studies are in progress to acquire SAR data on the role of various C-2 substituents and their effect on AChE-promoted Aβ aggregation.

2.4. SH-SY5Y neuroblastoma cell toxicity

The cytotoxicity of 2,4-disubstituted pyrimidine derivatives **7a, 7c, 7d, 7g, 7s, 7t, 8c** and **9c** was evaluated using a 3-(4,5-dimethylthiazol-2-yl)-2,5-diphenyl tetrazolium bromide (MTT) - based colorimetric assay. The cell viability of SH-SY5Y neuroblastoma cells after exposure to 2,4-disubstituted pyrimidines derivatives was compared with reference compounds tacrine and galanthamine (Table 3). At 40 μM, all the tested pyrimidine derivatives maintained efficient cell viability as measured by MTT reduction and were relatively nontoxic (Table 3). The *N*-benzyl derivative **7d** that exhibited selective AChE inhibition (IC_{50} = 24.9 μM) and excellent anti-aggregation activity (59% inhibition) was nontoxic (98% cell viability). For comparison, the viability of SH-SY5Y cells was 89% in the presence of the reference compound tacrine and 97% in the presence of the reference compound galanthamine under the same experimental conditions. In addition, the C-2 oxidized compounds **7s** (56% inhibition of Aβ-aggregation) and **7t** (44% inhibition of Aβ-aggregation) were only slightly toxic under these conditions, with cell viabilities of 90% and 92%, respectively. These studies indicate that the 2,4-disubstituted pyrimidines were nontoxic or only slightly toxic to SH-SY5Y cells and serve as a suitable template to develop ChEIs that exhibit activity against AChE-induced aggregation of Aβ.

2.5. Molecular modeling (docking) studies

Among the naphth-1-yl methyl series, the enzyme-ligand binding interactions of the most potent *h*AChE inhibitor **9a** [*N*-(naphth-1-ylmethyl)-2-(pyrrolidin-1-yl)pyrimidin-4-amine; *h*AChE IC_{50} = 5.5 μM; equine serum BuChE IC_{50} = 8.9 μM, SI = 0.62] within the active site of *h*AChE was investigated by molecular modeling studies (Figure 2). These investigations indicate that the central pyrimidine ring was approximately located midway through the active site gorge (~6 Å away from the catalytic triad His447 residue at the bottom of the active site and ~7 Å away from the PAS Trp286). The ring was also, (a) perpendicularly oriented between Trp86 and Phe297, (b) ~5 Å away from the hydrophobic pocket (Gly120–122) and (c) equidistantly stacked between Tyr124 and Tyr337. The latter feature allowed for two hydrogen bonding interactions between the tyrosine hydroxyl groups and the C-4 N*H* and two between the tyrosine hydroxyl groups and the pyrimidine N-3 (distances <3.5 Å). The C-4 naphth-1-yl ring was tightly stacked between Tyr337 and Trp86 (distance ~3.5 Å) and was in close proximity to His447 (distances 3.5–4 Å). The small C-2 pyrrolidine substituent was oriented toward an aromatic region close to the PAS (distance to Trp286 is ~4.5 Å) and was stacked beneath Tyr341 (distance ~3.5 Å). It is noteworthy that, although the catalytic site is relatively exposed in this binding pattern, the presence and location of the bulky C-4 naphth-1-yl ring most likely attribute to this derivative's potency considering the role that Trp86 plays in stabilizing the substrate ACh. This binding pattern is not seen in the related *N*-benzyl derivative **7a** (AChE IC_{50} = 8.7 μM), which re-enforces the unique dynamics offered by the naphth-1-yl methyl series of derivatives.

A similar docking experiment was conducted to investigate the binding interactions of the most potent and selective BuChE inhibitor **9e** [2-(4-methylpiperidin-1-yl)-*N*-(naphth-1-ylmethyl)pyrimidin-4-amine *h*AChE IC_{50} = 25.8 μM; BuChE IC_{50} = 2.2 μM, SI = 11.73) within the active site of *h*BuChE (Fig. 3). These studies indicate that the central pyrimidine ring was oriented (a) much closer to the catalytic active site (distance to His438 <3.5 Å), (b) was close to the hydrophobic pocket (Gly115–117; distance ~5 Å) and (c) was also perpendicularly stacked between Trp82 and Trp231. The C-4 naphth-1-yl methylamine group was oriented toward the acyl pocket (Leu286, Ser287 and Val288; distance ~4Å) and the naphth-1-yl ring was oriented toward an aromatic cage comprised of Trp231, Phe398 and Phe329. The C-4 N*H* was in close proximity to the catalytic residues (Ser198 and His438) and was undergoing hydrogen bonding interactions (distance <3 Å). The C-2 4-methylpiperidine substituent was oriented in an aromatic pocket comprised of Tyr440, Tyr332, Trp430 and Trp82. The shortest distance calculated between **9e** and the gorge entry residue

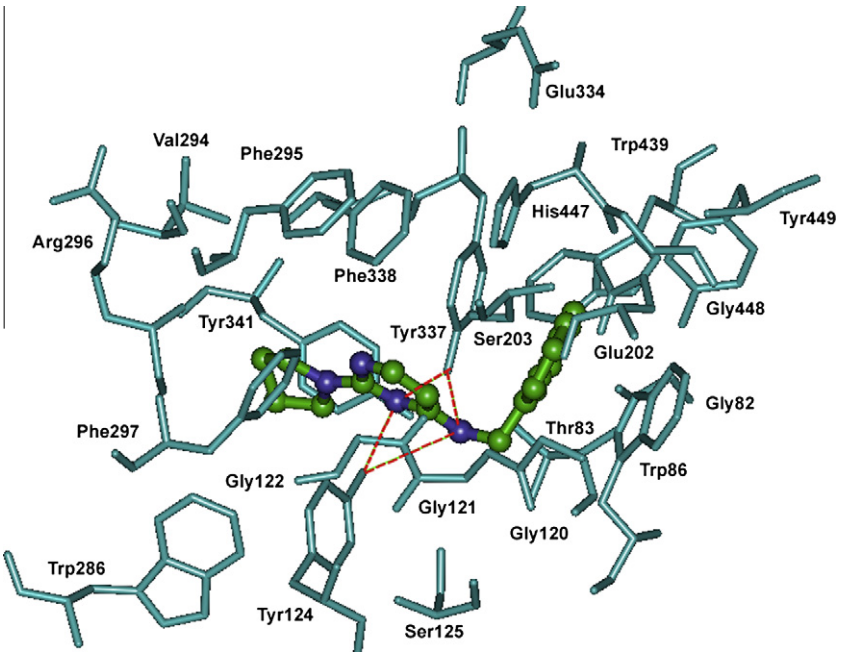

Figure 2. Docking of *N*-(naphthalen-1-ylmethyl)-2-(pyrrolidin-1-yl)pyrimidin-4-amine (**9a**, ball and stick) in the active site of *h*AChE. Red dotted lines represent hydrogen bonding. Hydrogen atoms are not shown for clarity.

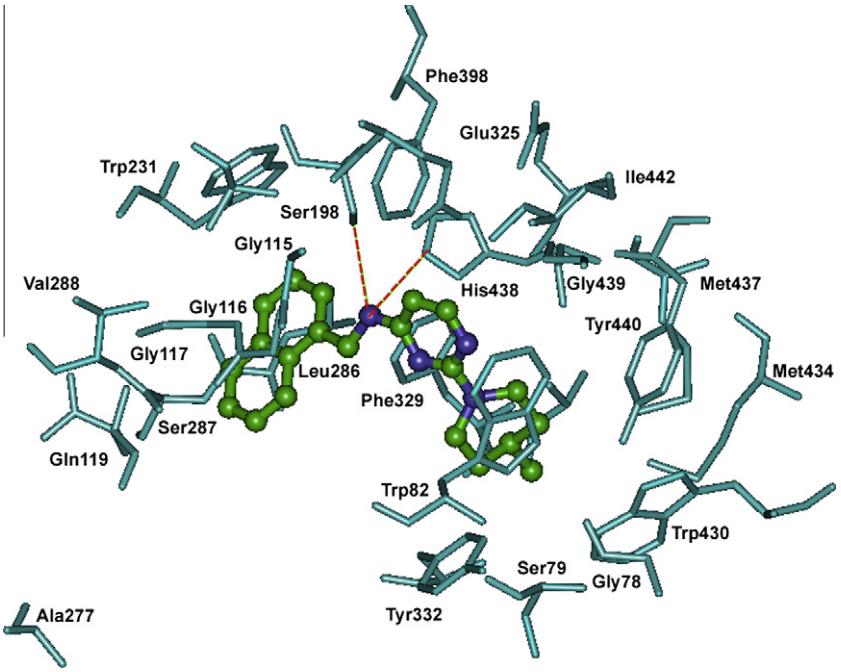

Figure 3. Docking of 2-(4-methylpiperidin-1-yl)-*N*-(naphthalen-1-yl methyl)pyrimidin-4-amine (**9e**, ball and stick) in the active site of *h*BuChE. Red dotted lines represent hydrogen bonding. Hydrogen atoms are not shown for clarity.

(Ala277) was ~10 Å, which reiterates the proximity of **9e** to the buried active site.

Furthermore, the similar BuChE inhibitory profiles of **9e** and its *N*-benzyl relative (**7e**, BuChE IC_{50} = 3.4; SI = 5.4) were investigated by superimposing the binding modes of both derivatives in *h*BuChE (Fig. 4). The superimposition revealed similar binding orientations within the active site where the larger naphth-1-ylmethyl C-4 group in **9e** occupies more room in the glycine hydrophobic pocket. Also, the C-2 methylpiperidine ring is planar to the pyrimidine ring in **7e** but perpendicular to the pyrimidine ring in **9e**. This is consistent with the fact that **9e** (volume = 231.9 $Å^3$, Supplementary data) has a bulkier C-4 (naphth-1-yl) substituent whereas **7e** consists of a less bulky phenyl ring at C-4 explaining the superior BuChE inhibitory potency exhibited by **9e** compared to **7e**.

3. Conclusions

The SAR data obtained on these novel class of 2,4-disubstituted pyrimidines indicates that (i) simple and efficient synthetic methods can be used to synthesize 2,4-disubstituted pyrimidines; (ii)

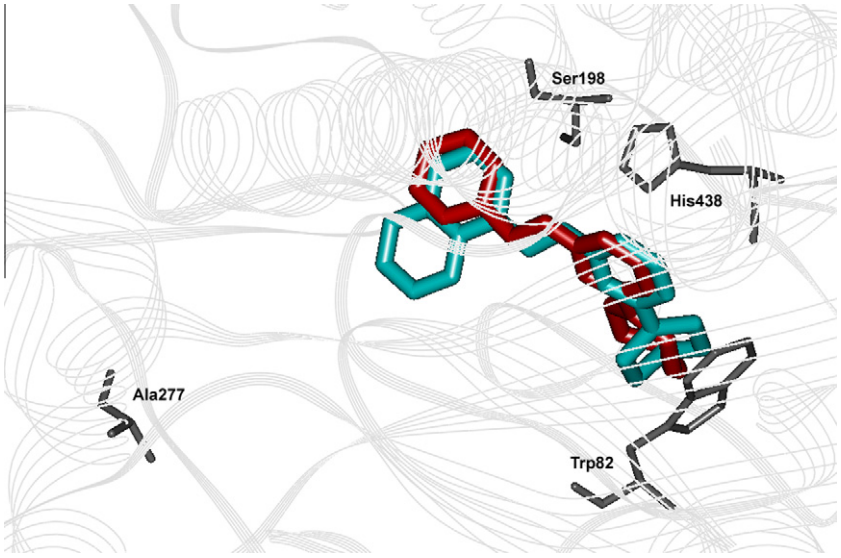

Figure 4. Superimposition of the binding modes of *N*-benzyl-2-(4-methylpiperidin-1-yl)pyrimidin-4-amine (**7e**, red) and 2-(4-methylpiperidin-1-yl)-*N*-(naphthalene-1-ylmethyl)pyrimidin-4-amine (**9e**, blue) within the active site of *h*BuChE.

the cholinesterase inhibition activity was sensitive to substituent steric and electronic properties at both C-2 and C-4 positions of the central pyrimidine ring; (iii) compound **9a** [*N*-(naphth-1-ylmethyl)-2-(pyrrolidin-1-yl)pyrimidin-4-amine] was identified as the most potent AChEI (IC_{50} = 5.5 μM), whereas **9e** [2-(4-methylpiperidin-1-yl)-*N*-(naphth-1-ylmethyl)pyrimidin-4-amine] was the most potent and selective BuChEI (IC_{50} = 2.2 μM, S.I = 11.73); (iv) **7d** containing a C-4 phenyl and a C-2 methylpiperidine acts as an AChEI and inhibits AChE-induced Aβ-aggregation; (v) 2,4-disubstituted pyrimidines could potentially serve as a suitable ring template to develop ChEIs that possess anti-Aβ aggregation activity and thus could target multiple pathological routes in AD.

4. Experimental section

4.1. General

Melting points were determined on a Fisher–Johns apparatus and are uncorrected. Infrared (IR) spectra were recorded as films on NaCl plates using a Perkin–Elmer FT-IR spectrometer. ^{1}H NMR spectra were recorded on a Bruker Avance 300 MHz series spectrometer ($CDCl_3$ as solvent). Coupling constants (*J* values) are in hertz (Hz). The following abbreviations are used for multiplicity of NMR signals: s = singlet, d = doublet, t = triplet, q = quartet, dd = double doublet, m = multiplet, br = broad. High-resolution electron ionization mass spectral (HREIMS) analysis was recorded using a JEOL HX110 double focusing mass spectrometer. Compound **7c** was synthesized from a previous literature report.[28] Combustion analysis was carried out by Midwest Microlab, LLC (Indianapolis, IN) and C, H, N of tested compounds **7a**–**t**, **8a**–**f** and **9a**–**e** were within ±0.4% of theoretical values for all elements listed indicating a purity of >95%. Silica gel column purification was performed using Merck 230–400 mesh Silica Gel 60. Compounds **7a**–**u**, **8a**–**f** and **9a**–**e** showed single spot on thin-layer chromatography (TLC) performed on Merck 60F254 silica gel plates (0.2 mm) using three different solvent systems (9:1 EtOAc/MeOH; 3:1 EtOAc/hexanes and 1:3 DCM/EtOAc) and spots were visualized with UV 254 nm or iodine. All other solvents and reagents were obtained from various vendors (Acros Organics, Sigma–Aldrich and Alfa Aesar) with a minimum purity of 95% and were used without further purification.

4.2. General procedure for the synthesis of 4-substituted-2-chloropyrimidin-4-amines (7–9)[28]

To a mixture of 2,4-dichloropyrimidine (**6**) (5.00 g, 33.60 mmol) and primary amines (33.60 mmol) in 65 mL of EtOH, kept at 0 °C (ice-bath), DIPEA (6.08 mL, 36.80 mmol) was added. The reaction was allowed to stir on the ice-bath for 5 minutes and was refluxed at 75–80 °C for 3 h. After cooling to 25 °C, the EtOH was evaporated in vacuo and the residue was re-dissolved in a solvent mixture of EtOAc and dichloromethane (DCM) in ~3:1 ratio and successfully washed with a concentrated $NaHCO_3$ and NaCl solution (1 × 15 mL). Aqueous layer was washed with EtOAc (3 × 15 mL) and the combined organic layer was dried over anhydrous $MgSO_4$ and filtered. The organic layer is evaporated in vacuo and the resulting residue was further purified using either one of the following two methods: (1) Method A: Silica gel column chromatography using EtOAc/hexanes twice (3:1 and 1:3, respectively) to afford solid products (60–65%); (2) Method B: Differential melting point separation—the collected organic layers are evaporated in vacuo and the oily residue is washed with a solution of hexanes and ether (~3:1) to afford a precipitate that was dried on filter paper at 80–85 °C for ~2 h to afford solid products. Some physical and spectroscopy data are provided below for **7**, **8** and **9**.

4.2.1. *N*-Benzyl-2-chloropyrimidin-4-amine (7)

The product was obtained as a white/light yellow solid after coupling with phenylmethaneamine (3.67 mL, 33.60 mmol). Method A—4.78 g, 65%; Method B—5.31 g, 72%. Mp: 130–132 °C; IR (film, CH_2Cl_2): 3434 cm^{-1} (NH); ^{1}H NMR (300 MHz, $CDCl_3$): δ 8.00 (d, *J* = 6.0 Hz, 1H), δ 7.28–7.34 (m, 5H), δ 6.20 (d, *J* = 6.0 Hz, 1H), δ 4.53 (br s, 2H). HREIMS calcd for $C_{11}H_{10}ClN_3$ (M^+) *m/z* 219.6702, observed 219.0498. Anal. Calcd for: $C_{11}H_{10}ClN_3 \cdot 0.32\ H_2O$; C, 58.55; H, 4.43, N, 18.63. Found: C, 58.61; H, 4.76; N, 18.64.

4.2.2. 2-Chloro-*N*-phenethylpyrimidin-4-amine (8)

The product was synthesized after coupling with 2-phenylethanamine (4.35 mL, 33.60 mmol). The residue is re-dissolved in a solvent mixture of EtOAc, DCM and MeOH in ~4:2:1 ratio. The resulting oily residue was further purified by silica gel column chromatography (Method A) to afford a white/off-white solid (4.70 g, 60%): mp: 75–77 °C. IR (film, CH_2Cl_2): 3433 cm^{-1} (NH);

^{1}H NMR (300 MHz, $CDCl_3$): δ 7.98 (d, J = 6.0 Hz, 1H), δ 7.17–7.33 (m, 5H), δ 6.16 (d, J = 6.0 Hz, 1H), δ 3.60 (br s, 2H), δ 2.88–2.92 (m, 2H). HREIMS calcd for $C_{12}H_{12}ClN_3$ (M^+) m/z 233.6968, observed 233.0606.

4.2.3. 2-Chloro-*N*-(naphth-1-ylmethyl)pyrimidin-4-amine (9)

The product was obtained after coupling with naphthalen-1-ylmethanamine (4.95 mL, 33.60 mmol) and was a light orange/brown solid (Method A—5.43 g, 60%; Method B—6.83 g, 75%): mp: 158–160 °C. IR (film, CH_2Cl_2): 3432 cm^{-1} (NH); ^{1}H NMR (300 MHz, $CDCl_3$): δ 8.01 (d, J = 6.0 Hz, 1H), δ 7.82–7.96 (m, 3H), δ 7.40–7.56 (m, 4H), δ 6.23 (d, J = 6.0 Hz, 1H) δ 4.70 (br s, 2H). HREIMS calcd for $C_{15}H_{12}ClN_3$ (M^+) m/z 269.7289, observed 269.0737. Anal. Calcd for: $C_{17}H_{18}ClN_3{\cdot}0.17H_20$: C, 66.79; H, 4.48, N, 15.58. Found: C, 66.04; H, 4.56; N, 15.40.

4.3. General procedure for the synthesis of 2,4-disubstituted-pyrimidin-4-amines (7a–r, 8a–f, 9a–e)[28]

To a solution of **7**, **8** or **9** (0.74–0.91 mmol) in 3 mL of *n*-BuOH kept in a PV with stirring, cyclic amines (1.12 mmol) was added. The sealed PV was placed in an oil bath at 145–150 °C and stirred for 30–40 min. *n*-BuOH was evaporated in vacuo and the residue was re-dissolved in 3:1 EtOAc/DCM and washed successively with saturated $NaHCO_3$ and NaCl solution (1 × 15 mL), respectively. The aqueous layer was washed with EtOAc (3 × 5 mL) and the organic layer was dried over anhydrous $MgSO_4$ then filtered. The solution was evaporated in vacuo to afford either solid or semisolid product. Some physical and spectroscopy data are provided below for **7a–r**, **8a–f, 9a–e**.

4.3.1. *N*-Benzyl-2-(pyrrolidin-1-yl)pyrimidin-4-amine (7a)

The product was obtained as a light brown solid after coupling **7** with pyrrolidine (0.15 g, 65%). Mp: 103–105 °C. IR (film, CH_2Cl_2): 3435 cm^{-1} (NH); ^{1}H NMR (300 MHz, $CDCl_3$): δ 7.87 (d, J = 6.0 Hz, 1H), δ 7.26–7.32 (m, 5H), δ 5.62 (d, J = 6.0 Hz, 1H), δ 4.86 (br s, 1H), δ 4.51 (d, J = 6.0 Hz, 2H), δ 3.49–3.53 (m, 4H), δ 1.90–1.94 (m, 4H). HREIMS calcd for $C_{15}H_{18}N_4$ (M^+) m/z 254.3302, found 254.1964. Anal. Calcd for: $C_{15}H_{18}N_4{\cdot}1H_2O$; C, 66.15; H, 7.40, N, 20.57. Found: C, 66.15; H, 7.40, N, 20.57.

4.3.2. *N*-Benzyl-2-morpholinopyrimidin-4-amine (7b)

The product was obtained after **7** coupling with morpholine (0.10 mL, 1.12 mmol) to afford an orange/light brown solid (0.20 g, 80%): mp: 93–95 °C. IR (film, CH_2Cl_2): 3434 cm^{-1} (NH); ^{1}H NMR (300 MHz, $CDCl_3$): δ 7.87 (d, J = 6.0 Hz, 1H), δ 7.29–7.31 (m, 5H), δ 5.69 (d, J = 6.0 Hz, 1H), δ 4.91 (br s, 1H), δ 4.50 (d, J = 6.0 Hz, 2H), δ 3.70–3.75 (m, 8H). HREIMS calcd for $C_{15}H_{18}N_4O$ (M^+) m/z 270.3296, found 270.1605. Anal. Calcd for $C_{15}H_{18}N_4O$: C, 66.64; H, 6.71, N, 20.73. Found: C, 66.45; H, 6.72; N, 20.46.

4.3.3. *N*-Benzyl-2-thiomorpholinopyrimidin-4-amine (7c)[28]

The product was obtained after **7** coupling with thiomorpholine (0.11 mL, 1.12 mmol) to afford an orange/light brown solid (0.20 g, 77%): mp: 85–87 °C. IR (film, CH_2Cl_2): 3258 cm^{-1} (NH); ^{1}H NMR (300 MHz, $CDCl_3$): δ 7.84 (d, J = 5.7 Hz, 1H), δ 7.24–7.33 (m, 5H), δ 5.66 (d, J = 5.7 Hz, 1H), δ 5.03 (br s, 1H), δ 4.47 (d, J = 5.6 Hz, 2H), δ 4.03–4.07 (m, 4H), δ 2.54–2.58 (m, 4H). HREIMS calcd for $C_{15}H_{18}N_4S$ (M^+) m/z 286.3952, found 286.1872. Anal. Calcd for $C_{15}H_{18}N_4S$: C, 62.91; H, 6.33, N, 19.56. Found: C, 62.62; H, 6.33; N, 19.31.

4.3.4. *N*-Benzyl-2-(4-methylpiperazin-1-yl)pyrimidin-4-amine (7d)

The product was obtained after coupling **7** with methylpiperazine (0.13 mL, 1.12 mmol) to afford a light yellow solid (0.22 g, 85%). Mp: 150–153 °C. IR (film, CH_2Cl_2): 3454 cm^{-1} (NH); ^{1}H NMR (300 MHz, $CDCl_3$): δ 7.86 (d, J = 6.0 Hz, 1H), δ 7.27–7.32 (m, 5H), δ 5.66 (d, J = 6.0 Hz, 1H), δ 4.87 (br s, 1H), δ 4.50 (d, J = 6.0 Hz, 2H), δ 3.77 (t, J = 6.0 Hz, 4H), δ 2.42 (t, J = 6.0 Hz, 4H), δ 2.31 (s, 3H). HREIMS calcd for $C_{16}H_{21}N_5$ (M^+) m/z 283.3714, found 283.1804. Anal. Calcd for $C_{16}H_{21}N_5{\cdot}0.6$EtOAc: C, 65.74; H, 7.74, N, 20.83. Found: C, 65.64; H, 7.75; N, 20.67.

4.3.5. *N*-Benzyl-2-(4-methylpiperidin-1-yl)pyrimidin-4-amine (7e)

The product was obtained after coupling **7** with methylpiperidine (0.14 mL, 1.12 mmol) to afford a whitish pink solid (0.22 g, 85%). Mp: 83–85 °C. IR (film, CH_2Cl_2): 3433 cm^{-1} (NH); ^{1}H NMR (300 MHz, $CDCl_3$): δ 7.85 (d, J = 6.0 Hz, 1H), δ 7.28–7.32 (m, 5H), δ 5.61 (d, J = 6.0 Hz, 1H), δ 4.84 (br s, 1H), δ 4.63–4.67 (m, 2H), δ 4.50 (d, J = 6.0 Hz, 2H), δ 2.73–2.81 (m, 2H), δ 1.62–1.66 (m, 2H), δ 1.22–1.26 (m, 1H), δ 1.10–1.18 (m, 2H), δ 0.91 (d, J = 6.0 Hz, 3H). HREIMS calcd for $C_{17}H_{22}N_4$ (M^+) m/z 282.3834, found 282.2376. Anal. Calcd for $C_{17}H_{22}N_4$: C, 72.31; H, 7.85, N, 19.84. Found: C, 72.18; H, 7.85; N, 19.60.

4.3.6. 1-[4-(4-(Benzylamino)pyrimidin-2-yl)piperazin-1-yl]ethanone (7f)

The product was obtained after coupling **7** with acetylpiperazine (0.15 g, 1.12 mmol) to afford a yellowish white solid (0.25 g, 86%). Mp: 150–153 °C. IR (film, CH_2Cl_2): 3437 cm^{-1} (NH); ^{1}H NMR (300 MHz, $CDCl_3$): δ 7.87 (d, J = 6.0 Hz, 1H), δ 7.28–7.31 (m, 5H), δ 5.70 (d, J = 6.0 Hz, 1H), δ 4.93 (br s, 1H), δ 4.49 (d, J = 6.0 Hz, 2H), δ 3.72–3.79 (m, 4H), δ 3.61–3.64 (m, 4H), δ 3.44–3.48 (m, 2H), δ 2.11 (s, 1H). HREIMS calcd for $C_{17}H_{21}N_5O$ (M^+) m/z 311.3815, found 311.1746. Anal. Calcd for $C_{17}H_{21}N_5O{\cdot}0.4$EtOAc: C, 64.46; H, 7.04, N, 20.21. Found: C, 64.43; H, 7.04; N, 20.15.

4.3.7. *tert*-Butyl 4-[4-(Benzylamino)pyrimidin-2-yl]piperazine-1-carboxylate (7g)

The product was obtained after coupling **7** with *tert*-butyl piperazine-1-carboxylate (0.22 g, 1.12 mmol). Product was purified using a 3:1 EtOAc/hexanes silica gel chromatography to afford a light yellowish solid (0.31 g, 90%). Mp: 115–117 °C. IR (film, CH_2Cl_2): 3438 cm^{-1} (NH); ^{1}H NMR (300 MHz, $CDCl_3$): δ 7.80 (d, J = 6.0 Hz, 1H), δ 7.21–7.30 (m, 5H), δ 5.65 (d, J = 6.0 Hz, 1H), δ 4.91 (br s, 1H), δ 4.49 (d, J = 6.0 Hz, 2H), δ 3.66–3.69 (m, 4H), δ 3.37–3.40 (m, 4H), δ 1.43 (s, 9H). HREIMS calcd for $C_{20}H_{27}N_5O$ (M^+) m/z 369.4607, found 369.2163. Anal. Calcd for $C_{20}H_{27}N_5O_2$: C, 65.02; H, 7.37, N, 18.96. Found: C, 65.54; H, 7.33; N, 18.76.

4.3.8. *N*-Benzyl-2-(4-cyclohexylpiperazin-1-yl)pyrimidin-4-amine (7h)

The product was obtained after coupling **7** with cyclohexylpiperazine (0.20 g, 1.12 mmol) and was purified using a 3:1 EtOAc/hexanes silica gel chromatography to afford an orange solid (0.21 g, 66%). Mp: 60–62 °C. IR (film, CH_2Cl_2): 3435 cm^{-1} (NH); ^{1}H NMR (300 MHz, $CDCl_3$): δ 7.82 (d, J = 6.0 Hz, 1H), δ 7.21–7.32 (m, 5H), δ 5.61 (d, J = 6.0 Hz, 1H), δ 5.07 (br s, 1H), δ 4.46 (d, J = 6.0 Hz, 2H), δ 3.72–3.75 (m, 4H), δ 2.54–2.57 (m, 4H), δ 2.25 (s, 1H), δ 1.86 (br s, 2H), δ 1.75 (br s, 2H), δ 1.58–1.61 (m, 1H), δ 1.13–1.19 (m, 5H). HREIMS calcd for $C_{21}H_{29}N_5$ (M^+) m/z 351.4885, found = 351.2259. Anal. Calcd for $C_{21}H_{29}N_5{\cdot}0.5$DCM: C, 65.55; H, 7.68, N, 17.78. Found: C, 65.77; H, 7.70; N, 17.85.

4.3.9. *N*-Benzyl-2-(4-isopropylpiperazin-1-yl)pyrimidin-4-amine (7i)

The product was obtained after coupling **7** with isopropylpiperazine (0.17 mL, 1.12 mmol) and was purified using a 3:1 EtOAc/hexanes silica gel chromatography to afford a white solid (0.14 g, 50%). Mp: 103–105 °C. IR (film, CH_2Cl_2): 3438 cm^{-1} (NH); ^{1}H

NMR (300 MHz, $CDCl_3$): δ 7.85 (d, J = 6.0 Hz, 1H), δ 7.24–7.34 (m, 5H), δ 5.63 (d, J = 6.0 Hz, 1H), δ 4.93 (br s, 1H), δ 4.48 (d, J = 6.0 Hz, 2H), δ 3.73–3.76 (m, 4H), δ 2.62–2.71 (m, 1H), δ 2.50–2.53 (m, 4H), δ 1.03 (d, J = 6.0 Hz, 6H). HREIMS calcd for $C_{18}H_{25}N_5$ (M^+) m/z 311.4246, found 311.2552. Anal. Calcd for $C_{18}H_{25}N_5$: C, 69.42; H, 8.09, N, 22.49. Found: C, 69.69; H, 8.31; N, 22.15.

4.3.10. *N*-Benzyl-2-(4-isopropylpiperidin-1-yl)pyrimidin-4-amine (7j)

The product was obtained after coupling **7** with isopropylpiperidine (0.17 mL, 1.12 mmol) and was purified using 3:1 ether/hexanes silica gel chromatography to afford a yellow solid (0.16 g, 55%). Mp: 58–60 °C. IR (film, CH_2Cl_2): 3438 cm^{-1} (NH); ^1H NMR (300 MHz, $CDCl_3$): δ 7.86 (d, J = 6.0 Hz, 1H), δ 7.22–7.32 (m, 5H), δ 5.61 (d, J = 6.0 Hz, 1H), δ 4.84 (br s, 1H), δ 4.71–4.75 (m, 2H), δ 4.49 (d, J = 6.0 Hz, 2H), δ 2.66–2.74 (m, 2H), δ 1.65–1.69 (m, 2H), δ 1.38–1.48 (m, 1H), δ 1.06–1.21 (m, 5H), δ 0.85–0.88 (m, 6H). HREIMS calcd for $C_{19}H_{26}N_4$ (M^+) m/z 310.4365, found 310.3086. Anal. Calcd for $C_{19}H_{26}N_4$: C, 73.51; H, 8.44, N, 18.05. Found: C, 73.51; H, 8.57; N, 17.91.

4.3.11. *N*-Benzyl-2-(4-propylpiperazin-1-yl)pyrimidin-4-amine (7k)

The product was obtained after coupling **7** with *n*-propylpiperazine (0.15 g, 1.12 mmol) and was purified using a 3:1 EtOAc/hexanes silica gel chromatography to afford a light orange solid (0.16 g, 55%). Mp: 93–95 °C. IR (film, CH_2Cl_2): 3436 cm^{-1} (NH); ^1H NMR (300 MHz, $CDCl_3$): δ 7.85 (d, J = 6.0 Hz, 1H), δ 7.21–7.30 (m, 5H), δ 5.64 (d, J = 6.0 Hz, 1H), δ 4.93 (br s, 1H), δ 4.48 (d, J = 6.0 Hz, 2H), δ 3.71–3.75 (m, 4H), δ 2.39–2.42 (m, 4H), δ 2.27–2.30 (m, 2H), δ 1.49–1.56 (m, 2H), δ 0.87–0.91 (m, 3H). HREIMS calcd for $C_{18}H_{25}N_5$ (M^+) m/z 311.4246, observed 311.2008. Anal. Calcd for $C_{18}H_{25}N_5{\cdot}0.6H_2O$: C, 67.09; H, 8.20, N, 21.73. Found: C, 67.11; H, 7.85; N, 21.55.

4.3.12. 2-[4-(4-(Benzylamino)pyrimidin-2-yl)piperazin-1-yl]ethanol (7l)

The product was obtained after coupling **7** with hydroxyethylpiperazine (0.14 mL, 1.12 mmol). Residue was re-dissolved in 1:1 EtOAc/DCM and was purified using a 3:1 EtOAc/hexanes silica gel chromatography to afford a brownish yellow solid (0.14 g, 50%). Mp: 103–105 °C. IR (film, CH_2Cl_2): 3439 cm^{-1} (NH); ^1H NMR (300 MHz, $CDCl_3$): δ 7.84 (d, J = 6.0 Hz, 1H), δ 7.24–7.34 (m, 5H), δ 5.65 (d, J = 6.0 Hz, 1H), δ 5.01 (br s, 1H), δ 4.48 (d, J = 6.0 Hz, 2H), δ 3.73–3.76 (m, 4H), δ 3.60–3.64 (m, 2H), δ 2.94 (s, 1H), δ 2.51–2.55 (m, 2H), δ 2.47–2.50 (m, 4H). HREIMS calcd for $C_{17}H_{23}N_5O$ (M^+) m/z 313.3974, found 313.1637. Anal. Calcd for $C_{17}H_{23}N_5O{\cdot}0.3DCM$: C, 60.20; H, 6.78, N, 20.65. Found: C, 60.03; H, 6.89; N, 20.10.

4.3.13. *N*-Benzyl-2-[4-(2-methoxyethyl)piperazin-1-yl]pyrimidin-4-amine (7m)

The product was obtained after coupling **7** with methoxyethylpiperazine (0.17 mL, 1.12 mmol) to afford an orange semi-solid (0.17 g, 57%). Mp: 63–65 °C. IR (film, CH_2Cl_2): 3433 cm^{-1} (NH); ^1H NMR (300 MHz, $CDCl_3$): δ 7.82 (d, J = 6.0 Hz, 1H), δ 7.21–7.31 (m, 5H), δ 5.62 (d, J = 6.0 Hz, 1H), δ 5.06 (br s, 1H), δ 4.46 (d, J = 6.0 Hz, 2H), δ 3.74–3.77 (m, 4H), δ 3.48–3.52 (m, 2H), δ 3.32 (s, 3H), δ 2.54–2.58 (m, 2H), δ 2.45–2.48 (m, 4H). HREIMS calcd for $C_{18}H_{25}N_5O$ (M^+) m/z 327.4240, found 327.2040.

4.3.14. *N*-Benzyl-2-[4-(4-chlorobenzyl)piperazin-1-yl]pyrimidin-4-amine (7n)

The product was obtained after coupling **7** with 4-chlorobenzylpiperazine (0.22 mL, 1.12 mmol). The sample was purified using a 9:1 EtOAc/DCM silica gel column to afford a yellowish solid (0.20 g, 55%). Mp: 88–90 °C. IR (film, CH_2Cl_2): 3437 cm^{-1} (NH); ^1H NMR (300 MHz, $CDCl_3$) δ 7.85 (d, J = 6.0 Hz, 1H), δ 7.24–7.30 (m, 9H), δ 5.65 (d, J = 6.0 Hz, 1H), δ 4.87 (br s, 1H), δ 4.48 (d, J = 6.0 Hz, 2H), δ 3.73–3.76 (m, 4H), δ 3.47 (s, 2H), δ 2.41–2.44 (m, 4H). HREIMS calcd for $C_{22}H_{24}ClN_5$ (M^+) m/z 393.9125, found 393.2443. Anal. Calcd for $C_{22}H_{24}ClN_5$: C, 67.08; H, 6.14, N, 17.78. Found: C, 67.44; H, 6.13; N, 17.68.

4.3.15. *N*-Benzyl-2-[4-(4-bromobenzyl)piperazin-1-yl]pyrimidin-4-amine (7o)

The product was obtained after coupling **7** with 4-bromobenzylpiperazine (0.29 g, 1.12 mmol) to afford a yellowish solid (0.20 g, 50%). Mp: 90–93 °C. IR (film, CH_2Cl_2): 3434 cm^{-1} (NH); ^1H NMR (300 MHz, $CDCl_3$) δ 7.85 (d, J = 6.0 Hz, 1H), δ 7.41–7.44 (m, 2H), δ 7.24–7.34 (m, 5H), δ 7.19–7.22 (m, 2H), δ 5.65 (d, J = 6.0 Hz, 1H), δ 4.87 (br s, 1H), δ 4.48 (d, J = 6.0 Hz, 2H), δ 3.73–3.76 (m, 4H), δ 3.45 (s, 2H), δ 2.41–2.44 (m, 4H). HREIMS calcd $C_{22}H_{24}BrN_5$ (M^+) m/z 438.3635, found 438.2430. Anal. Calcd for $C_{22}H_{24}BrN_5{\cdot}0.2EtOAc$: C, 60.06; H, 5.66, N, 15.36. Found: C, 60.07; H, 5.65; N, 15.39.

4.3.16. *N*-Benzyl-2-[4-(4-fluorobenzyl)piperazin-1-yl]pyrimidin-4-amine (7p)

The product was obtained after coupling **7** with 4-fluorobenzylpiperazine (0.22 g, 1.12 mmol) to afford an orange semi-solid (0.22 g, 65%). IR (film, CH_2Cl_2): 3439 cm^{-1} (NH); ^1H NMR (300 MHz, $CDCl_3$): δ 7.84 (d, J = 6.0 Hz, 1H), δ 7.26–7.29 (m, 7H), δ 6.96–7.02 (m, 3H), δ 5.63 (d, J = 6.0 Hz, 1H), δ 5.17 (br s, 1H), δ 4.47 (d, J = 6.0 Hz, 2H), δ 3.74–3.76 (m, 4H), δ 3.46 (s, 2H), δ 2.40 (t, J = 6.0 Hz, 4H). HREIMS calcd for $C_{22}H_{24}FN_5$ (M^+) m/z 377.4579, found 377.1980. Anal. Calcd for $C_{22}H_{24}FN_5{\cdot}0.5DCM$: C, 64.36; H, 6.00, N, 16.68. Found: C, 63.95; H, 5.97; N, 16.54.

4.3.17. *N*-Benzyl-2-[4-(4-trifluoromethylbenzyl)piperazin-1-yl]pyrimidin-4-amine (7q)

The product was obtained after coupling **7** with 4-trifluoromethybenzylpiperazine (0.24 mL, 1.12 mmol) to afford a yellowish orange solid (0.25 g, 64%). Mp: 88–90 °C. IR (film, CH_2Cl_2): 3437 cm^{-1} (NH). ^1H NMR (300 MHz, $CDCl_3$): δ 7.85 (d, J = 6.0 Hz, 1H), δ 7.55–7.58 (m, 2H), δ 7.44–7.47 (m, 2H), δ 7.24–7.34 (m, 5H), δ 5.65 (d, J = 6.0 Hz, 1H), δ 5.00 (br s, 1H), δ 4.48 (d, J = 6.0 Hz, 2H), δ 3.75–3.78 (m, 4H), δ 3.55 (s, 2H), δ 2.43–2.46 (m, 4H). HREIMS calcd $C_{23}H_{24}F_3N_5$ (M^+) m/z 427.4654, found 427.2203. Anal. Calcd for $C_{23}H_{24}F_3N_5$: C, 64.62; H, 5.66, N, 16.38. Found: C, 64.39; H, 5.64; N, 16.12.

4.3.18. N^4-Benzyl-N^2-(1-benzylpiperidin-4-yl)pyrimidine-2,4-diamine (7r)

The product was obtained after coupling **7** with 4-amino-1-benzylpiperidine (0.23 mL, 1.12 mmol) to afford a dark orange solid (0.20 g, 59%). Mp: 88–90 °C. IR (film, CH_2Cl_2): 3438 cm^{-1} (NH). ^1H NMR (300 MHz, $CDCl_3$): δ 7.78 (d, J = 6.0 Hz, 1H), δ 7.21–7.34 (m, 10H), δ 5.66 (d, J = 6.0 Hz, 1H), δ 4.92 (br s, 1H), δ 4.46 (d, J = 6.0 Hz, 2H), δ 3.76–3.82 (m, 1H), δ 3.48 (s, 2H), δ 2.76–2.80 (m, 2H), 2.09–2.16 (m, 2H), 1.95–1.99 (m, 3H), 1.42–1.55 (m, 2H). HREIMS calcd $C_{23}H_{27}N_5$ (M^+) m/z 373.4940, found 373.2008. Anal. Calcd for $C_{23}H_{27}N_5{\cdot}DCM$: C, 62.88; H, 6.38, N, 15.28. Found: C, 62.88; H, 6.38; N, 15.28.

4.3.19. *N*-Phenethyl-2-(pyrrolidin-1-yl)pyrimidin-4-amines (8a)

The product was obtained by coupling **8** with pyrrolidine to afford a light yellowish brown solid (0.15 g, 65%). Mp: 85–87 °C. IR (film, CH_2Cl_2): 3436 cm^{-1} (NH); ^1H NMR (300 MHz, $CDCl_3$): δ 7.86 (d, J = 6.0 Hz, 1H), δ 7.18–7.32 (m, 5H), δ 5.59 (d, J = 6.0 Hz, 1H), δ 4.56 (br s, 1H), δ 3.55 (t, J = 6.0 Hz, 2H), δ 3.50 (t, J = 6.0 Hz, 4H), δ 2.86–2.91 (m, 2H), δ 1.90–1.93 (m, 4H). HREIMS $C_{16}H_{20}N_4$

(M^+) *m/z* 268.3568, found 268.2125. Anal. Calcd for $C_{16}H_{20}N_4{\cdot}0.5H_2O$: C, 69.29; H, 7.63, N, 20.2. Found: C, 69.51; H, 7.32; N, 20.11.

4.3.20. 2-Morpholino-*N*-phenethylpyrimidin-4-amine (8b)

The product was obtained after coupling **8** with morpholine (0.10 mL, 1.11 mmol) to afford a light brown solid (0.21 g, 86%). Mp: 93–95 °C. IR (film, CH_2Cl_2): 3433 cm^{-1} (NH); ^1H NMR (300 MHz, $CDCl_3$): δ 7.85 (d, J = 6.0 Hz, 1H), δ 7.18–7.32 (m, 5H), δ 5.65 (d, J = 6.0 Hz, 1H), δ 4.59 (br s, 1H), δ 3.68–3.75 (m, 8H), δ 3.55–3.59 (m, 2H), δ 2.86–2.90 (m, 2H). HREIMS calcd $C_{16}H_{20}N_4O$ (M^+) *m/z* 284.3562, found 284.1725. Anal. Calcd for $C_{16}H_{20}N_4O$: C, 67.58; H, 7.09, N, 19.70. Found: C, 67.71; H, 7.14; N, 19.42.

4.3.21. *N*-Phenethyl-2-thiomorpholinopyrimidin-4-amine (8c)

The product was obtained after coupling **8** with thiomorpholine (0.11 mL, 1.11 mmol) to afford a brown solid (0.21 g, 81%). Mp: 60–62 °C. IR (film, CH_2Cl_2): 3437 cm^{-1} (NH); ^1H NMR (300 MHz, $CDCl_3$) δ 7.84 (d, J = 6.0 Hz, 1H), δ 7.18–7.30 (m, 5H), δ 5.61 (d, J = 6.0 Hz, 1H), δ 4.58 (br s, 1H), δ 3.98 (t, J = 6.0 Hz, 4H), δ 3.54 (t, J = 6.0 Hz, 2H), δ 2.86–2.90 (m, 2H), δ 2.61 (t, J = 6.0 Hz, 4H). HREIMS calcd $C_{16}H_{20}N_4S$ (M^+) *m/z* 284.3562, found 284.1725. Anal. Calcd for $C_{16}H_{20}N_4S$: C, 63.97; H, 6.71, N, 18.65. Found: C, 64.12; H, 6.85; N, 18.46.

4.3.22. 2-(4-Methylpiperazin-1-yl)-*N*-phenethylpyrimidin-4-amine (8d)

The product was obtained after coupling **8** with methylpiperazine (0.12 mL, 1.11 mmol) to afford a light yellow semi-solid (0.18 g, 69%). Mp: 58–60 °C IR (film, CH_2Cl_2): 3436 cm^{-1} (NH); ^1H NMR (300 MHz, $CDCl_3$): δ 7.85 (d, J = 6.0 Hz, 1H), δ 7.18–7.30 (m, 5H), δ 5.62 (d, J = 6.0 Hz, 1H), δ 4.57 (br s, 1H), δ 3.76–3.79 (m, 4H), δ 3.52–3.56 (m, 2H), δ 2.86–2.90 (m, 2H), δ 2.41–2.44 (m, 4H), δ 2.31 (s, 3H). HREIMS calcd $C_{17}H_{23}N_5$ (M^+) *m/z* 297.3980, found 297.1958. Anal. Calcd for: $C_{17}H_{23}N_5{\cdot}13\ H_2O$; C, 68.05; H, 7.67, N, 23.35. Found: C, 68.12; H, 7.82; N, 23.36.

4.3.23. 2-(4-Methylpiperidin-1-yl)-*N*-phenethylpyrimidin-4-amine (8e)

The product was obtained after coupling **8** with 4-methylpiperidine (0.13 mL, 1.11 mmol) to afford a light brown solid (0.20 g, 79%). Mp: 65–67 °C. IR (film, CH_2Cl_2): 3439 cm^{-1} (NH); ^1H NMR (300 MHz, $CDCl_3$): δ 7.84 (d, J = 6.0 Hz, 1H), δ 7.18–7.33 (m, 5H), δ 5.57 (d, J = 6.0 Hz, 1H), δ 4.64–4.69 (m, 2H), δ 4.53 (br s, 1H), δ 3.52–3.56 (m, 2H), δ 2.86–2.90 (m, 2H), δ 2.73–2.82 (m, 2H), δ 1.63–1.68 (m, 3H), δ 1.33–1.40 (m, 1H), δ 1.08–1.16 (m, 3H), δ 0.92 (d, J = 6.0 Hz, 3H). HREIMS calcd $C_{18}H_{24}N_4$ (M^+) *m/z* 296.4100, found 296.2380. Anal. Calcd for $C_{18}H_{24}N_4$: C, 72.94; H, 8.16, N, 18.90. Found: C, 72.38; H, 7.99; N, 18.34.

4.3.24. 1-[4-(4-(Phenethylamino)pyrimidin-2-yl)piperazin-1-yl]ethanone (8f)

The product was obtained after coupling **8** with acetylpiperazine (0.14 g, 1.11 mmol) to afford a yellow solid (0.24 g, 86%). Mp: 150–152 °C. IR (film, CH_2Cl_2): 3437 cm^{-1} (NH); ^1H NMR (300 MHz, $CDCl_3$): δ 7.85 (d, J = 6.0 Hz, 1H), δ 7.19–7.33 (m, 5H), δ 5.66 (d, J = 6.0 Hz, 1H), δ 4.61 (br s, 1H), δ 3.73–3.80 (m, 4H), δ 3.65 (t, J = 6.0 Hz, 2H), δ 3.55 (t, J = 6.0 Hz, 2H), δ 3.46–3.50 (m, 2H), δ 2.86–2.90 (m, 2H), δ 2.12 (s, 3H). HREIMS calcd $C_{18}H_{23}N_5O$ (M^+) *m/z* 325.4081, found 325.1913. Anal. Calcd for $C_{18}H_{23}N_5{\cdot}0.6EtOAc$: C, 64.78; H, 7.41, N, 18.52. Found: C, 64.66; H, 7.43; N, 18.30.

4.3.25. *N*-(Naphth-1-ylmethyl)-2-(pyrrolidine)pyrimidin-4-amines (9a)

The product was obtained after coupling **9** with pyrrolidine to afford a light brown solid (0.16 g, 70%). Mp: 105–107 °C. IR (film, CH_2Cl_2): 3433 cm^{-1} (NH); ^1H NMR (300 MHz, $CDCl_3$) δ 8.05 (d, J = 6.0 Hz, 1H), δ 7.78–7.91 (m, 3H), δ 7.38–7.51 (m, 4H), δ 5.64 (d, J = 6.0 Hz, 1H), δ 4.96 (d, J = 6.0 Hz, 2H), δ 4.79 (br s, 1H), δ 3.53–3.57 (m, 4H), δ 1.91–1.95 (m, 4H). HREIMS calcd $C_{19}H_{20}N_4$ (M^+) *m/z* 304.3889, found 304.2086. Anal. Calcd for $C_{19}H_{20}N_4{\cdot}0.2H_2O$: C, 74.02; H, 6.49, N, 18.18. Found: C, 74.09; C, 6.68; N, 18.19.

4.3.26. 2-Morpholino-*N*-(naphth-1-ylmethyl)pyrimidin-4-amine (9b)

The product was obtained after coupling **9** with morpholine (0.08 mL, 0.96 mmol) to afford a light yellow solid (0.18 g, 75%). Mp: 170–172 °C. IR (film, CH_2Cl_2): 3437 cm^{-1} (NH); ^1H NMR (300 MHz, $CDCl_3$): δ 8.01 (d, J = 6.0 Hz, 1H), δ 7.79–7.90 (m, 3H), δ 7.39–7.52 (m, 4H), δ 5.71 (d, J = 6.0 Hz, 1H), δ 4.92 (d, J = 6.0 Hz, 2H), δ 4.77 (br s, 1H), δ 3.69–3.77 (m, 8H). HREIMS calcd $C_{19}H_{20}N_4O$ (M^+) *m/z* 320.3883, found 320.1825. Anal. Calcd for $C_{19}H_{20}N_4O$: C, 71.23; H, 6.29, N, 17.49. Found: C, 71.28; H, 6.37; N, 17.08.

4.3.27. *N*-(Naphth-1-ylmethyl)-2-thiomorpholinopyrimidin-4-amine (9c)

The product was obtained after coupling **9** thiomorpholine (0.10 mL, 0.96 mmol) to afford a yellowish brown solid (0.19 g, 76%). Mp: 105–107 °C. IR (film, CH_2Cl_2): 3439 cm^{-1} (NH); ^1H NMR (300 MHz, $CDCl_3$): δ 8.01 (d, J = 6.0 Hz, 1H), δ 7.73–7.87 (m, 3H), δ 7.39–7.51 (m, 4H), δ 5.68 (d, J = 6.0 Hz, 1H), δ 4.93 (d, J = 6.0 Hz, 2H), δ 4.82 (br s, 1H), δ 4.05–4.12 (m, 4H), δ 2.59–2.65 (m, 4H). HREIMS calcd $C_{19}H_{20}N_4S$ (M^+) *m/z* 336.4539, found 336.2171. Anal. Calcd for $C_{19}H_{20}N_4S$: C, 67.83; H, 5.99, N, 16.65. Found: C, 67.78; H, 5.86; N, 16.50.

4.3.28. 2-(4-Methylpiperazin-1-yl)-*N*-(naphth-1-ylmethyl)pyrimidin-4-amine (9d)

The product was obtained after coupling **9** with methylpiperazine (0.11 mL, 0.96 mmol) to afford a yellow solid (0.23 g, 80%). Mp: 118–120 °C. IR (film, CH_2Cl_2): 3436 cm^{-1} (NH); ^1H NMR (300 MHz, $CDCl_3$): δ 8.03 (d, J = 6.0 Hz, 1H), δ 7.78–7.90 (m, 3H), δ 7.39–7.52 (m, 4H), δ 5.67 (d, J = 6.0 Hz, 1H), δ 4.94 (d, J = 6.0 Hz, 2H), δ 4.80 (br s, 1H), δ 3.81–3.85 (m, 4H), δ 2.41–2.45 (m, 4H), δ 2.32 (s, 3H). HREIMS calcd $C_{20}H_{23}N_5$ (M^+) *m/z* 333.4301, found 333.1961. Anal. Calcd for $C_{20}H_{23}N_5{\cdot}0.5EtOAc$: C, 70.01; H, 7.21, N, 18.55. Found: C, 69.72; H, 7.25; N, 18.21.

4.3.29. 2-(4-Methylpiperidin-1-yl)-*N*-(naphth-1-ylmethyl)pyrimidin-4-amine (9e)

The product was obtained after coupling **9** with 4-methylpiperidine (0.11 mL, 0.96 mmol). The residue was purified using 3:1 ether/hexanes column to afford an off-white/light yellow semi-solid (0.14 g, 55%). IR (film, CH_2Cl_2): 3439 cm^{-1} (NH); ^1H NMR (300 MHz, $CDCl_3$): δ 8.03 (d, J = 6.0 Hz, 1H), δ 7.78–7.91 (m, 3H), δ 7.38–7.53 (m, 4H), δ 5.62 (d, J = 6.0 Hz, 1H), δ 4.94 (d, J = 6.0 Hz, 2H), δ 4.75 (br s, 1H), δ 4.68–4.72 (m, 3H), δ 2.76–2.84 (m, 2H), δ 1.64–1.68 (m, 2H), 1.57–1.60 (m, 1H), 1.10–1.14 (m, 4H), 0.92 (d, J = 6.0 Hz, 3H). HREIMS calcd $C_{21}H_{24}N_4$ (M^+) *m/z* 332.4421, found 332.2246. Anal. Calcd for $C_{21}H_{24}N_4{\cdot}0.5EtOAc$: C, 73.38; H, 7.50, N, 14.88. Found: C, 73.07; H, 7.52; N, 14.64.

4.4. Preparation of 4-[4-(benzylamino)pyrimidin-2-yl]thiomorpholine-1-oxide (7s)

To a mixture of *N*-benzyl-2-thiomorpholinopyrimidin-4-amine (**7c**) (0.20 g, 0.70 mmol) in 4 mL of 1,4-dioxane, kept at 0 °C (ice-bath), *m*CPBA (0.19 g, 1.12 mmol) was added dropwise. The reaction is allowed to stir on the ice-bath for 5 min and then was kept at rt for 3 h. DCM was added to the mixture to aid in the 1,4-

dioxane in vacuo evaporation. The residue was re-dissolved in a solvent mixture of EtOAc and DCM in ~3:1 ratio and successfully washed with a concentrated $NaHCO_3$ and NaCl solution (1 × 15 mL). Aqueous layer was washed with EtOAc (3 × 15 mL) and the combined organic layer was dried over anhydrous $MgSO_4$ and filtered. The organic layer was evaporated in vacuo and the resulting solid residue was further purified by silica gel column chromatography using 3:1 EtOAc/hexanes to afford a light yellow solid (0.16 g, 75%). Mp: 78–80 °C. IR (film, CH_2Cl_2): 3439 cm^{-1} (NH); ^1H NMR (300 MHz, $CDCl_3$): δ 7.87 (d, J = 6.0 Hz, 1H), δ 7.24–7.35 (m, 5H), δ 5.74 (d, J = 6.0 Hz, 1H), δ 4.99 (br s, 1H), δ 4.49 (d, J = 6.0 Hz, 2H), δ 4.37 (t, J = 6.0 Hz, 1H), δ 4.32 (t, J = 6.0 Hz, 1H), 4.10–4.19 (m, 2H), 2.69–2.73 (m, 4H). HREIMS calcd $C_{15}H_{18}N_4OS$ (M^+) m/z 302.3946, found 302.1259. Anal. Calcd for $C_{15}H_{18}N_4OS$·0.3DCM: C, 56.05; H, 5.72, N, 17.09. Found: C, 56.38; H, 5.74; N, 17.22.

4.5. Preparation of 4-[4-(benzylamino)pyrimidin-2-yl]thiomorpholine-1,1-dioxide (7t)

To a mixture of *N*-benzyl-2-thiomorpholinopyrimidin-4-amine (**7c**) (0.20 g, 0.70 mmol) in 5 mL of MeOH, kept at 0 °C (ice-bath), potassium peroxymonosulphate (0.23 g, 1.54 mmol) in H_2O was added dropwise. The reaction was allowed to stir on the ice-bath for 5 min and then was kept at 70–75 °C for 1 h. Four milliliters of 1,4-dioxane were added to the mixture and the reaction vessel was moved to rt for 4 h. MeOH and 1,4-dioxane were evaporated in vacuo and the residue was re-dissolved in 3:1 EtOAc/DCM and successfully washed with a concentrated $NaHCO_3$ and NaCl solution (1 × 15 mL). Aqueous layer was washed with EtOAc (3 × 15 mL) and the combined organic layer was dried over anhydrous $MgSO_4$ and filtered. The organic layer was evaporated in vacuo and the resulting solid residue was further purified by silica gel column chromatography using 3:1 EtOAc/hexanes to afford a light orange solid (0.17 g, 75%). Mp: 65–67 °C. IR (film, CH_2Cl_2): 3464 cm^{-1} (NH); ^1H NMR (300 MHz, $CDCl_3$): δ 7.87 (d, J = 6.0 Hz, 1H), δ 7.25–7.35 (m, 5H), δ 5.79 (d, J = 6.0 Hz, 1H), δ 5.14 (br s, 1H), δ 4.49 (d, J = 6.0 Hz, 2H), δ 4.21–4.25 (m, 4H), δ 2.88–2.92 (m, 4H), 4.10–4.19 (m, 2H), 2.69–2.73 (m, 4H). HREIMS calcd $C_{15}H_{10}N_4O_2S$ (M^+) m/z 318.3946, found 318.1310. Anal. Calcd for $C_{15}H_{18}N_4OS_2$·0.2DCM: C, 51.95; H, 5.28, N, 15.94. Found: C, 52.04; H, 5.34; N, 15.71.

4.6. Preparation of *N*-benzyl-2-(piperazin-1-yl)pyrimidin-4-amine (7u)

To a mixture of *tert*-butyl 4-(4-(benzyl amino)pyrimidin-2-yl)piperazine-1-carboxylate (**7g**) (0.20 g, 0.54 mmol) in 4 mL of DCM, kept at 0 °C (ice-bath), TFA (4 mL, 53.83 mmol) was added dropwise. The reaction was allowed to stir on the ice-bath for 5 min and then was kept at rt for 2 h. DCM is evaporated in vacuo and the residue was re-dissolved in 3:1 EtOAc/DCM and successfully washed with a concentrated $NaHCO_3$ and NaCl solution (1 × 15 mL). Aqueous layer was washed with EtOAc (3 × 15 mL) and the combined organic layer was dried over anhydrous $MgSO_4$ and filtered. The organic layer was evaporated in vacuo to afford a light yellow solid (0.11 g, 75%). Mp: 70–72 °C. IR (film, CH_2Cl_2): 3438 cm^{-1} (NH); ^1H NMR (300 MHz, $CDCl_3$): δ 7.86 (d, J = 6.0 Hz, 1H), δ 7.24–7.34 (m, 5H), δ 5.66 (d, J = 6.0 Hz, 1H), δ 4.91 (br s, 1H), δ 4.49 (d, J = 6.0 Hz, 2H), δ 3.73–3.76 (m, 4H), 3.09 (s, 1H), δ 2.88–2.91 (m, 4H). HREIMS calcd $C_{15}H_{19}N_5$ (M^+) m/z 269.3449, found 269.1953.

4.7. Cholinesterase inhibition assay

The ability of the test compounds (**7a**–**u**, **8a**–**f** and **9a**–**e**) to inhibit human AChE (product number C3389, Sigma-Aldrich, St. Louis, MO) and equine serum BuChE (product number C1057, Sigma-Aldrich, St. Louis, MO) was determined using Ellman's method (IC_{50} values, μM) using appropriate reference agents tacrine hydrochloride (item number 70240, Cayman Chemical, Ann Arbor, MI), bis(7)-tacrine (item number 10005836, Cayman Chemical, Ann Arbor, MI), and galanthamine hydrobromide (product number G1660, Sigma, St. Louis, MO). Stock solutions of test compounds were dissolved in a minimum volume of DMSO (1%) and were diluted using the buffer solution (50 mM Tris–HCl, pH 8.0, 0.1 M NaCl, 0.02 M $MgCl_2·6H_2O$). In 96-well plates, 160 μL 5,5′-dithiobis(2-nitrobenzoic acid) (1.5 mM DTNB), 50 μL of AChE (0.22 U/mL prepared in 50 mM Tris–HCl, pH 8.0, 0.1% w/v bovine serum albumin, BSA) or 50 μL of BuChE (0.06 U/mL prepared in 50 mM Tris–HCl, pH 8.0, 0.1% w/v BSA) were incubated with 10 μL of various concentrations of test compounds (0.001–100 μM) at room temperature for 5 min followed by the addition of the substrates (30 μL) acetylthiocholine iodide (15 mM ATCl) or *S*-butyrylthiocholine iodide (15 mM BTCI) and the absorbance was measured at different time intervals (0, 60, 120 and 180 s) at a wavelength of 405 nm BioTek ELx800 microplate reader. Percent inhibition was calculated by the comparison of compound treated to various control incubations that included 1% DMSO. The concentration of the test compound causing 50% inhibition (IC_{50}, μM) was calculated from the concentration–inhibition response curve on logarithmic scale (duplicate to quadruplicate determinations).

4.8. *h*AChE-induced Aβ aggregation inhibition studies

Thioflavin T (ThT) is a benzothiazole salt frequently used in the detection of amyloid plaque formation. As Aβ peptides start to aggregate into oligomers and fibrils, ThT binds to the beta sheets formed as a result of the aggregation and the detectable change in its emission spectrum is used to quantify the degree of aggregation.[32–34] $A\beta_{1-40}$ was purchased from GL Biochem Ltd. Human recombinant AChE lyophilized powder was purchased from Sigma Aldrich (product number C1682) and ThT was purchased from Fisher Scientific. $A\beta_{1-40}$ was prepared as previously described.[32] Lyophilized $A\beta_{1-40}$ was dissolved in DMSO to obtain a 2 mM solution and then diluted into 500 μM solution with 0.215 M sodium phosphate buffer (pH 8.0). Aliquots (2 μL) of $A\beta_{1-40}$ were incubated with 16 μL of *h*AChE, which was dissolved in 0.215 M sodium phosphate buffer (pH 8.0), to give a final concentration of 50 μM of $A\beta_{1-40}$ and 230 μM of *h*AChE. For co-incubation experiments, 2 μL of the test compounds in 0.215 M sodium phosphate buffer pH 8.0 solution (final concentration 100 μM) were added into aliquots (2 μL) of $A\beta_{1-40}$ (final concentration 50 μM) along with 16 μL of *h*AChE (final concentration 230 μM). The reaction mixtures were incubated at room temperature for 24 h and 100 μL of ThT (20 μM) in 50 mM glycine-NaOH buffer (pH 8.5) was added. Fluorescence was monitored at 442 nm and emission at 490 nm using a Proton Technology International (PTI, Birmingham, NJ) spectrofluorometer. Each assay was run in triplicates along with donepezil (item number 13245, Caymen Chemical, Ann Arbor, MI) and propidium iodide (product number C4170, Sigma–Aldrich, St. Louis, MO) as reference agents. The fluorescence intensities in the presence and absence of inhibitors were compared using appropriate controls containing 1% DMSO and the percentage of inhibition was calculated using the equation: $100 - (IF_i/IF_o \times 100)$ where IF_i and IF_o are the fluorescence intensities obtained for $A\beta_{1-40}$ + *h*AChE in the presence and absence of inhibitor, respectively.

4.9. SH-SY5Y neuroblastoma cell toxicity studies

The cellular reduction of 3-(4,5-dimethylthiazol-2-yl)-2,5-diphenyl tetrazolium bromide, MTT (Product No. 30-1010K, from American Type Culture Collection, Manassas, VA) was measured

by detecting a purple formazan intermediate at 570 nm. By incubating the cells with varying concentrations of test compounds, their toxicity attributes can be determined directly by determining the %reduction of MTT or indirectly by reporting the %viability of the cell line used.[35,36] The SH-SY5Y neuroblastoma cells were plated at a density of 50,000 cells per well in 100 μL of complete media consisting of a 1:1 mixture of Eagle's Minimum Essential Medium (EMEM) and Ham's F12, supplemented with 10% Fetal Bovine Serum (FBS). The cells were incubated overnight before treatment with 100 μL of test sample solutions and select controls (tacrine hydrochloride, item number 70240, Caymen Chemical, Ann Arbor, MI and galanthamine hydrobromide, product number G1660 Sigma–Aldrich, St. Louis, MO) at various concentrations (0–160 μM) in 2% DMSO for 24 h at 37 °C ($n = 4$). A 20 μL of the MTT reagent solution was added and the cells were incubated for an additional 3 h. The cells were subsequently solubilized with 80 μL of MTT reagent solution and incubated at room temperature overnight. Cell viability was determined by measuring the absorbance at 570 nm using a Molecular Devices Spectramax 190 microplate reader. All results were expressed as a percent reduction of MTT relative to untreated controls that included 2% DMSO (defined as 100% viability) and the average absorbance value for each treatment was subtracted with the absorbance reading of wells containing only media, MTT reagent, and detergent reagent.

4.10. Molecular modeling (docking) studies

Docking experiments were performed using Discovery Studio Client v2.5.0.9164 (2005-09), Accelrys Software Inc. running on a HP xw4600 workstation (Processor x86 family 6 model 23 stepping 10 GenuineIntel 2999 MHz). The coordinates for the X-ray crystal structure of the enzyme *h*AChE and *h*BuChE were obtained from the RCSB Protein Data Bank and hydrogens were added. The ligand molecules were constructed using the Build Fragment tool and energy minimized for 1000 iterations reaching a convergence of 0.01 kcal/mol Å. The docking experiment on *h*AChE was carried out by superimposing the energy minimized ligand in the PDB file 1B41 after which fasciculin was deleted. The coordinates for *h*BuChE was obtained from PDB file 1P0I and the energy minimized ligand was superimposed and the resulting ligand–enzyme complex was subjected to docking using the Libdock command in the receptor–ligand interactions protocol of Discovery Studio after defining subsets of the enzyme within 10 Å sphere radius of the ligand. The force field, Chemistry at HARvard Macromolecular Mechanics (CHARMM) was employed for all docking purposes. The ligand–enzyme assembly was then subjected to a molecular dynamics (MD) simulation using Simulation protocol at a constant temperature of 300 K with a 100 step equilibration for over 1000 iterations and a time step of 1 fs using a distance dependent dielectric constant 4*r*. The optimal binding orientation of the ligand–enzyme assembly obtained after docking was further minimized for 1000 iterations using the conjugate gradient method until a convergence of 0.001 kcal/mol Å was reached after which $E_{\text{intermolecular}}$ (kcal/mol) of the ligand–enzyme assembly was evaluated.

Acknowledgments

The authors would like to thank the Department of Biology and the School of Pharmacy at the University of Waterloo for financial support of this research project. This work was also partially supported by the Alzheimer's Association (NIRG-08-91651) and the Alzheimer's Disease Research Center (NIH 3P50 AG005131). The NSF is also acknowledged for a CAREER Award to JY (CHE-0847530).

Supplementary data

Supplementary data [a table of molecular volume (Å^3) for some compounds are given] associated with this article can be found, in the online version, at doi:10.1016/j.bmc.2011.02.030.

References and notes

1. Holden, M.; Kelly, C. *Adv. Psychiatr. Treat.* **2002**, *8*, 89.
2. Klafki, H.; Staufenbiel, M.; Kornhuber, J.; Wiltfang, J. *Brain* **2006**, *129*, 2840.
3. Edwards, P. D.; Albert, J. S.; Sylvester, M.; Aharony, D.; Andisik, D.; Callaghan, O.; Campbell, J. B.; Carr, R. A.; Chessari, G.; Congreve, M.; Frederickson, M.; Folmer, R. H. A.; Geschwindner, S.; Koether, G.; Kolmodin, K.; Krumrine, J.; Mauger, R. C.; Murray, C. W.; Olsson, L.; Patel, S.; Spear, N.; Tian, G. *J. Med. Chem.* **2007**, *50*, 5912.
4. Selkoe, D. J. *Science* **2002**, *298*, 789.
5. Aguzzi, A.; O'Conner, T. *Nat. Rev. Drug Disc.* **2010**, *9*, 237.
6. Melnikova, I. *Nat. Rev. Drug Disc.* **2007**, *6*, 341.
7. Suh, W. H.; Suslick, K. S.; Suh, Y. *Curr. Med. Chem.* **2005**, *5*, 259.
8. Shen, T.; Tai, K.; Henchman, R. H.; McCammon, J. A. *Acc. Chem. Res.* **2002**, *35*, 340.
9. Darvesh, S.; Hopkins, D. A.; Geula, C. *Nat. Rev. Neurosci.* **2003**, *4*, 131.
10. Green, K. D.; Fridman, M.; Garneau-Tsodikova, S. *ChemBioChem* **2009**, *10*, 2191.
11. Soreq, H.; Seidman, S. *Nat. Rev. Neurosci.* **2001**, *2*, 294.
12. Villalobos, A.; Blake, J. F.; Biggers, C. K.; Butler, T. W.; Chapin, D. S.; Chen, Y. L.; Ives, J. L.; Jones, S. B.; Liston, D. R.; Nagel, A. A.; Nason, D. M.; Neilson, J. A.; Shalaby, I. A.; White, W. F. *J. Med. Chem.* **1994**, *37*, 2721.
13. Kamal, M. A.; Qu, X.; Yu, Q.; Tweedie, D.; Holloway, H. W.; Li, Y.; Tan, Y.; Greig, N. H. *J. Neural. Trans.* **2008**, *115*, 889.
14. Campiani, G.; Fattorusso, C.; Butini, S.; Gaeta, A.; Agnusdei, M.; Gemma, S.; Persico, M.; Catalanotti, B.; Savini, L.; Nacci, V.; Novellino, E.; Holloway, H. W.; Greig, N. H.; Belinskaya, T.; Fedorko, J. M.; Saxena, A. *J. Med. Chem.* **2005**, *48*, 1919.
15. Gibbs, M. E.; Maksel, D.; Gibbs, Z.; Hou, X.; Summers, R. J.; Small, D. H. *Neurobiol. Aging* **2010**, *31*, 614.
16. Dinamarca, M. C.; Sagal, J. P.; Quintanilla, R. A.; Godoy, J. A.; Arrazola, M. S.; Inestrosa, N. C. *Mol. Neurodegener.* **2010**, *5*, 2.
17. Rosini, M.; Simoni, E.; Bartolini, M.; Cavalli, A.; Ceccarini, L.; Pascu, N.; McClymont, D. W.; Tarozzi, A.; Bolognesi, M. L.; Minarini, A.; Tumiatti, V.; Andrisano, V.; Mellor, I. R.; Melchiorre, C. *J. Med. Chem.* **2008**, *51*, 4381.
18. Pakaski, M.; Kalman, J. *Neurochem. Int.* **2008**, *53*, 103.
19. Racchi, M.; Mazzucchelli, M.; Lenzken, S. C.; Porrello, E.; Lanni, C.; Govoni, S. *Chem. Biol. Interact.* **2005**, *157–158*, 335.
20. Inestrosa, N. C.; Dinamarca, M. C.; Alvarez, A. *FEBS J.* **2008**, *275*, 625.
21. Inestrosa, N. C.; Alvarez, A.; Perez, C. A.; Moreno, R. D.; Vincete, M.; Linker, C.; Casanueva, O. I.; Soto, C.; Garrido, J. *Neuron* **1996**, *16*, 881.
22. Belluti, F.; Rampa, A.; Piazzi, L.; Bisi, A.; Gobbi, S.; Bartolini, M.; Andrisano, V.; Cavalli, A.; Recanatini, M.; Valenti, P. *J. Med. Chem.* **2005**, *48*, 4444.
23. Harel, M.; Schalk, I.; Ehret-Sabatier, L.; Bouet, F.; Goeldner, M.; Hirth, C.; Axelsen, P. H.; Silman, I.; Sussman, J. L. *Proc. Natl. Acad. Sci. U.S.A.* **1993**, *90*, 9031.
24. Pang, P.; Quiram, P.; Jelacic, T.; Hong, F.; Brimijoin, S. *J. Biol. Chem.* **1996**, *271*, 23646.
25. Bolognesi, M. L.; Andrisano, V.; Bartolini, M.; Banzi, R.; Melchiorre, C. *J. Med. Chem.* **2005**, *48*, 24.
26. Greenblatt, H. M.; Silman, I.; Sussman, J. L. *Drug Dev. Res.* **2000**, *50*, 573.
27. Lee, L. L.; Ha, H.; Chang, Y.; Delisa, M. P. *Protein Sci.* **2009**, *18*, 277.
28. Mohamed, T.; Rao, P. P. N. *Bioorg. Med. Chem. Lett.* **2010**, *20*, 3606.
29. Nugiel, D. A.; Cornelius, L. A. M.; Corbett, J. W. *J. Org. Chem.* **1997**, *62*, 201.
30. Fiorini, M. T.; Abell, C. *Tetrahedron Lett.* **1998**, *39*, 1827.
31. Ellman, G. L.; Courtney, K. D.; Andres, V. *Biochem. Pharmacol.* **1961**, *7*, 88.
32. Zhao, X.; Yang, J. *ACS Chem. Neurosci.* **2010**, *1*, 655.
33. Khurana, R.; Coleman, C.; Ionescu-Zanetti, C.; Carter, S. A.; Krishna, V.; Grover, R. K.; Roy, R.; Singh, S. *J. Struct. Biol.* **2005**, *151*, 229.
34. Eubanks, L. M.; Rogers, C. J.; Beuscher, A. E., IV; Koob, G. F.; Olson, A. J.; Dickerson, T. J.; Janda, K. D. *Mol. Pharm.* **2006**, *3*, 773.
35. Mosmann, T. *J. Immunol. Methods* **1983**, *65*, 55.
36. Vellonen, K.; Honkakoski, P.; Urtti, A. *Eur. J. Pharm. Sci.* **2004**, *23*, 181.